TITLE PAGE
MODIFICATION OF CATALYST FOR BIODIESEL PRODUCTION

USING SOL-GEL METHOD

BY

IGBINEHI GODSWILL OSAIGBOVO

ENG2002039

DEPARTMENT OF CHEMICAL ENGINEERING,

FACULTY OF ENGINEERING,

UNIVERSITY OF BENIN,

BENIN CITY

OCTOBER\, 2025

CERTIFICATION

This is to certify that this project research was carried out by **IGBINEHI GODSWILL OSAIGBOVO** of the Department of Chemical Engineering at the University of Benin, Benin city, Edo State, Nigeria.

——————————————— ———————————————

PROF. E.A OYEDOH **DATE**

PROJECT SUPERVISOR

——————————————— ———————————————

PROF. S.E UWADIAE **DATE**

PROJECT COORDINATOR

——————————————— ———————————————

PROF. E.A OYEDOH **DATE**

HEAD OF DEPARTMENT

——————————————— ———————————————

EXTERNAL EXAMINER **DATE**

DEDICATION

I dedicate this project to God Almighty, whose love and grace carried me through every step. To my late father, **Mr. Daniel Osariemen Igbinehi**, whose sacrifices lit the path for my education, and whose memory inspires me daily. To my beloved mother **Mrs Betty Igbinehi**, whose unwavering support and endless love held me up through every challenge. To my dear siblings, **Marvis, Destiny, and Precious Igbinehi**, whose support, presence and encouragement filled my days with joy. To my precious grandmother, Imayuse Omosigho, and my late great-grandmother, **Omwanghe Uhunmwangho**, whose blessings and wisdom guide me still. To my incredible aunties and uncles, Mrs. Caroline Omorowa, Mr. Victor Omosigho, Mrs. Justina Okundaye, Mr. Uyi Omisigho, and Mrs. Josephine Omoruyi, whose care and belief in me warmed my heart. To my brother and friend, Lawson Okundaye, who stood by me throughout the struggle and triumph. And to my amazing cousins, Imade Omoruwa, Brooks Okundaye, Wesley Okundaye, Oduwa Izevbuwa, Malcolm Okundaye, Mrs Faith Asemota, Etinosa Omoruyi, Jude Omorowa, and all my relatives at home and abroad, whose love and prayers wrapped me in strength. This work is a tribute to you all, my family, my home.

ACKNOWLEDGEMENT

With a heart full of gratitude, I first thank **God** Almighty for His boundless love, strength, and guidance throughout this project journey. I am deeply grateful to my project supervisor, **Prof. E.A. Oyedoh**, whose wisdom and encouragement shaped this work. My heartfelt thanks go to Mr. David Ahonkhai for his unwavering support and constant guidance, which kept me grounded. I sincerely appreciate my lab instructor, Engr. Fred Oshomogho, for his expertise and patience in the laboratory. To my dear friend Emmanuel Agho, thank you for always being there to help me navigate challenges in the lab—your kindness made all the difference.

I extend my gratitude to the Church of Christ Iwogban 2 Congregation, especially my preacher, Mr. Peter Akhigbe, and his lovely, Mrs. Joy Akhigbe, for their prayers and spiritual support. My thanks also go to the Church of Christ Uniben/UBTH for their uplifting presence, your encouragement warmed my heart and kept me going.

I am immensely grateful to my amazing coursemates, Emmanuel Victor, Jeffrey Oshionubu, our diligent course representative David Asani, Ifeoma Beci, Precious Anesi, Christabel Omene, Godson Otaigbe, Agnes, Kenneth, Da silva, sylvester, wisdom, Henry, Godwin, Paul and everyone else, for your support and kindness. Finally, I thank every lecturer and staff member of the Chemical Engineering Department for their knowledge and guidance, your collective support turned this journey into a valued experience.

ABSTRACT

This study investigated the production of biodiesel from waste cooking oil using a catalyst derived from chicken manure impregnated with nickel sulfate. The catalyst was prepared by calcining chicken manure followed by a sol-gel process to incorporate nickel, and characterized as a porous material with a surface area of 115 m^2/g. Using Response Surface Methodology, the reaction conditions were optimized, identifying a methanol-to-oil ratio of 12:1, 3% catalyst loading, 55°C temperature, and 90 minutes reaction time as optimal, resulting in a biodiesel yield of 95.67%. The biodiesel met flash point safety standards but showed higher viscosity, density, and acid value than international fuel specifications, indicating the presence of residual free fatty acids that require pretreatment or purification. This work demonstrates that chicken manure can serve as a cost-effective catalyst precursor in converting waste cooking oil to biodiesel, promoting sustainable waste utilization and renewable energy production.

TABLE OF CONTENT

Contents

LIST OF TABLES

LIST OF FIGURES

LIST OF PLATES

NOMENCLATURE

Abbreviations and Acronyms

- **ASTM**: American Society for Testing and Materials
- **BBD**: Box-Behnken Design
- **BET**: Brunauer-Emmett-Teller
- **CCD**: Central Composite Design
- **CVD**: Chemical Vapor Deposition
- **C.V.**: Coefficient of Variation
- **DA**: Dubinin-Astakhov
- **df**: Degrees of Freedom
- **DRIFTS**: Diffuse Reflectance Infrared Fourier Transform Spectroscopy
- **EDX / EDS**: Energy-Dispersive X-ray Spectroscopy
- **FAEE**: Fatty Acid Ethyl Esters
- **FAME**: Fatty Acid Methyl Esters
- **FFD**: Full Factorial Design
- **FID**: Flame Ionization Detector
- **FTIR (FT-IR)**: Fourier Transform Infrared Spectroscopy
- **GC**: Gas Chromatography
- **JCPDS**: Joint Committee on Powder Diffraction Standards
- **MOCVD**: Metal-Organic Chemical Vapor Deposition
- **MOFs**: Metal-Organic Frameworks
- **RSM**: Response Surface Methodology
- **SEM**: Scanning Electron Microscopy
- **TEOS**: Tetraethyl Orthosilicate
- **UCO**: Used Cooking Oil
- **WCO**: Waste Cooking Oil
- **XRD**: X-ray Diffraction
- **XRF**: X-ray Fluorescence

2. Symbols and Notations

- **A, B, C, D**: Factors in RSM (Methanol/oil ratio, Catalyst loading, Reaction temperature, Reaction time)
- **a0** : Constant term in RSM model
- **ai ,aii ,aij** : Linear, quadratic, and interaction regression coefficients in RSM model
- **AIS** : Peak area of the internal standard
- **Al**: Aluminum
- **Al2 O3** : Aluminum Oxide (Alumina)
- **b,B**: Volume of blank titrant
- **Ba**: Barium
- **BaSO4** : Baryte (Barium Sulfate)
- **c,N**: Normality of titrant
- **C**: Carbon
- **Ca**: Calcium
- **Ca2+**: Calcium ion
- **CaCO3** : Calcium Carbonate
- **Ca(OH)2** : Calcium Hydroxide
- **CaO**: Calcium Oxide
- **CaSO4 ·2H2 O**: Gypsum
- **Ca3 (PO4)2** : Calcium Phosphate
- **CeO2** : Cerium Oxide
- **CH3 OH**: Methanol
- **cm−1**: Wavenumber (unit)
- **cm3/g**: Cubic centimeters per gram (unit for pore volume)
- **CO2** : Carbon Dioxide
- **CIS** : Concentration of the internal standard
- **C2 H5 OH**: Ethanol
- **dV(d)**: Differential pore volume
- **ϵ**: Experimental model error

- **Fe**: Iron
- **Fe2 O3** : Iron(III) Oxide
- **g/cm3 (or g/ml)**: Grams per cubic centimeter (unit for density)
- **H2** : Hydrogen
- **H2 O**: Water
- **H2 SO4** : Sulfuric Acid
- **H3 PO4** : Phosphoric Acid
- **HCl**: Hydrochloric Acid
- **K**: Kelvin (unit of temperature)
- **K+**: Potassium ion
- **K2 O**: Potassium Oxide
- **KAlSi3 O8** : Sanidine
- **KI**: Potassium Iodide
- **kJmol−1**: Kilojoules per mole (unit of energy)
- **KOH**: Potassium Hydroxide
- **kV**: Kilovolts
- **λ**: Wavelength
- **m,W**: Mass of sample
- **M**: Molarity (mol/L)
- **m2/g (or m2g−1)**: Square meters per gram (unit for surface area)
- **mEq/Kg**: Milliequivalents per kilogram (unit for peroxide value)
- **mg KOH/g**: Milligrams of KOH per gram (unit for acid value)
- **Mg**: Magnesium
- **MgO**: Magnesium Oxide
- **MJ kg−1**: Megajoules per kilogram (unit of energy)
- **mm2/s**: Square millimeters per second (unit for kinematic viscosity)
- **Mn**: Manganese
- **MnO**: Manganese Oxide
- **M−O−M**: Metal-Oxygen-Metal linkage
- **N1,N2**: Titre value for sample and blank
- **Na**: Sodium

- **Na2 CO3** : Sodium Carbonate
- **Na2 S2 O3** : Sodium Thiosulfate
- **NH4 OH**: Ammonium Hydroxide
- **(NH4)2 Ni(SO4)2 ·6H2 O**: Nickelboussingaultite
- **NiO**: Nickel Oxide
- **NiSO4 ·6H2 O**: Nickel Sulphate Hexahydrate
- **nm**: Nanometers (unit of length)
- **O2−**: Oxide ion
- **P**: Phosphorus
- **P/P0** : Relative Pressure
- **P2 O5** : Phosphorus Pentoxide
- **R2**: Coefficient of Determination
- **ROH**: Alcohol
- **R′COOR**: Fatty Acid Alkyl Ester (Biodiesel)
- **rpm**: Revolutions per minute
- **v,S**: Volume of sample titrant
- **V**: Volume of KOH titrant
- **VIS** : Volume of the internal standard
- **wt%**: Weight percent
- **Xi ,Xj** : Independent variables (factors) in RSM model
- **Y**: Predicted response (Biodiesel Yield)
- **Zn**: Zinc
- **ZnO**: Zinc Oxide
- **Zr**: Zirconium
- **ZrO2** : Zirconium Dioxide
- **∑A**: Total peak area of FAMEs

CHAPTER ONE

INTRODUCTION

1.1 BACKGROUND STUDY

Biodiesel, a renewable and environmentally friendly fuel, has gained significant attention as an alternative to fossil fuels because of its ability to reduce greenhouse gas emissions and dependence on non-renewable resources. Biodiesel is typically produced through the transesterification of vegetable oils or animal fats with alcohols, such as methanol or ethanol, in the presence of a catalyst. Traditional homogeneous catalysts, such as sodium hydroxide and sulfuric acid, have been widely used but pose significant challenges, including the generation of large amounts of wastewater, the need for neutralization, and difficulties in product separation, which increase both costs and environmental impact (Teo et al. 2014).

Among the various sources of heterogeneous catalysts, biomass-derived materials have emerged as promising candidates owing to their abundance, low cost, and sustainability. Chicken manure, an abundant agricultural waste, has gained attention as a potential source of heterogeneous catalysts. It is rich in minerals such as calcium, phosphorus, and magnesium, which can be converted into catalysts. When doped with transition metals, such as nickel, chicken manure can be transformed into an effective catalyst for biodiesel production. Nickel-based catalysts are particularly valuable because of their high activity in transesterification reactions, as they facilitate the formation of active sites that enhance the reaction process (Obahiagbon and Ahonkhai 2023). For instance, Obahiagbon and Ahonkhai (2023) demonstrated that nickel (II) nitrate-doped chicken manure achieved a biodiesel yield of 99.4026% under optimized conditions, highlighting its potential.

Chicken manure is a promising precursor for catalyst synthesis due to its high nutrient content, particularly nitrogen, phosphorus, potassium, and trace metals like calcium and magnesium. These elements are essential for forming active catalytic sites, especially in metal oxide-based catalysts. The manure's organic matter also contributes to structural properties, such as porosity, which are beneficial for catalytic applications (Andrayani, Sangkala, and Susilawati 2024; Nainggolan et al. 2025).

Pretreatment is critical to prepare chicken manure for conversion into metal oxides. Common methods include thermal treatments, such as pyrolysis, to remove organic impurities and concentrate inorganic components. Hydrothermal and enzymatic pretreatments are also used to enhance nutrient availability and reduce contaminants like heavy metals and antibiotics (Kucuker, Demirel, and Onay 2020; Ranzi et al. 2018). These steps improve the carbon-to-nitrogen ratio and optimize the material for catalytic applications (Konkol, Świerczek, and Cenian 2023)

However, challenges remain. Variability in manure composition due to factors like chicken diet and housing conditions can affect consistency. Additionally, heavy metals and residual antibiotics in manure pose risks, requiring careful pretreatment to ensure safe and effective catalyst production (Wang et al. 2017). Despite these challenges, chicken manure-derived catalysts have shown potential in biodiesel production, offering a sustainable use for agricultural waste.

Catalysts play a pivotal role in biodiesel production by enhancing reaction rates and improving yields. The modification of catalysts using advanced techniques like sol-gel and hydrothermal methods has been shown to significantly improve their structural and chemical properties, such as surface area, porosity, and active site distribution. These improvements are critical for achieving high biodiesel yields and ensuring the reusability of the catalyst ((Rahman, 2019); (Mohadesi, 2014)).

Advanced synthesis techniques, such as sol-gel and hydrothermal methods, are crucial for preparing catalysts with desired properties. The sol-gel method involves the formation of a colloidal suspension (sol) that evolves into a gel, which is then dried and calcined to produce a catalyst with high homogeneity and a large surface area.

Making use of sol-gel method can further enhance the properties of catalysts. For instance, catalysts prepared using a sol-gel route exhibit larger surface areas, better porosity, and improved catalytic performance. This synergy is particularly beneficial for biodiesel production, where both esterification and transesterification reactions require catalysts with high activity and stability (Xu et al. 2008).

Traditional catalysts, such as sodium hydroxide, create waste and are difficult to separate; therefore, scientists are looking at greener options, such as catalysts from chicken manure, which

is rich in minerals, such as calcium and phosphorus. The addition of nickel sulphate, a transition metal, can boost the catalyst performance. Methods such as sol-gel (mixing chemicals to form a gel) can make these catalysts more effective by improving their surface area and structure.

The use of advanced catalyst modification techniques not only improves the efficiency of biodiesel production but also reduces the environmental impact by enabling the use of waste materials as feedstocks. This aligns with global efforts to develop sustainable and cost-effective energy solutions (Cheng and Li 2018).

1.2 STATEMENT OF THE PROBLEM

Despite the potential of biomass-derived catalysts, there is a notable gap in research concerning the use of chicken manure modified with nickel sulphate via sol-gel method for biodiesel production. While studies have explored chicken manure as a catalyst source, particularly for calcium-based catalysts, the specific application of these advanced synthesis techniques to incorporate nickel sulphate remains underexplored (Maroa and Inambao 2021; Obahiagbon and Ahonkhai 2023). This gap limits the development of sustainable and cost-effective catalysts that can enhance the efficiency of biodiesel production processes. For instance, while Jung et al. (2019) explored CO_2-mediated chicken manure biochar manipulation for biodiesel, they did not focus on nickel sulphate or advanced synthesis methods, leaving a research gap. Addressing this gap is essential for advancing the field of renewable energy and promoting sustainable waste utilization.

While chicken manure has been studied as a catalyst, the use of sol-gel method with nickel sulphate has been less explored. This gap implies that the efficacy of these method in developing efficient and eco-friendly catalysts for biodiesel, which is crucial for sustainable energy, remains unclear.

1.3 AIM AND OBJECTIVES

Aim:

The primary aim of this study was to develop effective bio based catalyst from chicken manure doped with nickel sulphate using sol-gel method .

Objectives:

1. The physicochemical properties of waste cooking oil, including free fatty acid content, viscosity, and moisture content, will be characterized to establish its suitability for biodiesel production.

2. Nickel sulphate-doped chicken manure catalysts will be synthesized using sol-gel method and the preparation conditions will be optimized for enhanced catalytic performance.

3. The structural, morphological, and chemical properties of the catalysts will be analyzed using X-ray diffraction (XRD), Brunauer-Emmett-Teller (BET) analysis, Fourier transform infrared spectroscopy (FT-IR), scanning electron microscopy (SEM), and energy-dispersive X-ray spectroscopy (EDS).

4. Biodiesel will be produced through the transesterification of waste cooking oil with methanol using the prepared catalysts under controlled reaction conditions.

5. To optimize the biodiesel production process, parameters such as the methanol-to-oil ratio, catalyst loading, reaction temperature, and time will be varied using response surface methodology (RSM) to maximize the yield.

6. The produced biodiesel will be characterized for key properties, including fatty acid methyl ester (FAME) content, density, viscosity, and flash point, using gas chromatography (GC) and standard ASTM methods to ensure compliance with biodiesel quality standards.

1.4 SCOPE OF STUDY

This study focuses on the synthesis, characterization, and performance evaluation of nickel sulphate-doped chicken manure catalysts for biodiesel production. The catalyst is prepared using the sol-gel method, which involves the formation of a gel-like network through chemical reactions. This method are chosen for its ability to produce catalysts with high surface area, porosity, and active site distribution, which are critical for efficient biodiesel production (Moradi et al. 2015; Rahman et al. 2019).

The study employs waste cooking oil as the feedstock for biodiesel production, addressing the dual challenge of waste management and renewable energy generation. The transesterification reaction is carried out using methanol, with the synthesized catalysts facilitating the conversion of triglycerides into fatty acid methyl esters (FAME). The reaction parameters, such as methanol-to-oil molar ratio, reaction temperature, catalyst loading, and reaction time, are systematically optimized to maximize biodiesel yield (Farouk et al. 2024; Godarzi et al. 2023).

The scope of this research is limited to laboratory-scale experiments, excluding pilot-scale or industrial applications. This limitation is informed by the need to establish proof-of-concept and to evaluate the feasibility of using chicken manure as a sustainable catalyst precursor. Similar studies have demonstrated the effectiveness of lab-scale testing in providing valuable insights into catalyst performance and process optimization (Moradi et al. 2015; Sakti La Ore et al. 2020)

The study also includes a detailed characterization of the catalysts using techniques such as BET surface area analysis, X-ray diffraction (XRD), scanning electron microscopy (SEM), and Fourier-transform infrared spectroscopy (FTIR). These analyses aim to correlate the structural and chemical properties of the catalysts with their catalytic performance.

1.5 SIGNIFICANCE OF THE STUDY

This study is important for several reasons. First, it addresses the valorization of chicken manure, an abundant agricultural waste, by transforming it into a valuable catalyst for biodiesel production. This approach not only reduces waste but also contributes to environmental sustainability by promoting the use of renewable resources, aligning with the principles of a circular economy (Maroa and Inambao 2021). Second, the development of efficient catalyst

using advanced synthesis methods, such as sol-gel technique, can enhance the efficiency of biodiesel production processes, reducing both costs and environmental impact compared to traditional homogeneous catalysts. For instance, Obahiagbon and Ahonkhai (2023) reported high biodiesel yields with nickel-doped chicken manure, suggesting cost-effectiveness. The findings of this study could provide valuable insights into the design and optimisation of biomass-derived catalysts, which may have applications beyond biodiesel production, such as in other catalytic processes, such as syngas production. Furthermore, by advancing the technology for biodiesel production, this study supports the global transition towards renewable energy sources, helping to mitigate the environmental challenges associated with fossil fuel dependence (Teo et al. 2014).

CHAPTER TWO
LITERATURE REVIEW

2.1 INTRODUCTION

Biodiesel production has gained global attention as a renewable and environmentally friendly alternative to conventional petroleum diesel. However, the economic viability and large-scale adoption of biodiesel are strongly influenced by the type and performance of catalysts used in its synthesis (Atabani et al., 2022). Traditional homogeneous catalysts such as sodium hydroxide (NaOH) and potassium hydroxide (KOH) offer high conversion efficiencies but suffer from drawbacks including difficulty in separation, soap formation, and poor reusability (Chouhan & Sarma, 2020).

To overcome these limitations, researchers have increasingly focused on heterogeneous catalysts, particularly those derived from biowaste and agricultural residues, due to their low cost, sustainability, and abundance of catalytically active components such as calcium oxide (CaO), magnesium oxide (MgO), and potassium oxide (K_2O) (Li et al., 2023). Among these, chicken manure is an especially attractive raw material because of its high calcium content, ease of availability, and potential for waste valorization (Adepoju & Akintunde, 2024).

Nevertheless, raw or unmodified chicken-manure-based catalysts often exhibit low surface area, poor thermal stability, and leaching of active species, leading to reduced catalytic efficiency and poor reusability (Ogunkunle & Ahmed, 2021). These challenges have motivated the application of catalyst modification techniques such as sol–gel and hydrothermal methods to enhance textural, chemical, and catalytic properties (Li et al., 2023).

This chapter reviews relevant literature on biodiesel production and catalysts, focusing on the development and modification of chicken-manure-derived catalysts through sol–gel and hydrothermal synthesis techniques. The review aims to provide a conceptual understanding of how these modification routes influence catalyst performance, process efficiency, and biodiesel yield (Atabani et al., 2022; Adepoju & Akintunde, 2024).

2.2 BIODIESEL: AN OVERVIEW

Biodiesel is a renewable, biodegradable, and non-toxic fuel composed mainly of mono-alkyl esters of long-chain fatty acids obtained through the transesterification or esterification of lipids such as vegetable oils, animal fats, or microbial oils with a short-chain alcohol, most commonly methanol or ethanol, in the presence of a suitable catalyst (Atabani et al., 2022; Li et al., 2023). Chemically, biodiesel is represented as fatty acid methyl esters (FAME) or fatty acid ethyl esters (FAEE) depending on the alcohol used. The overall reaction converts triglycerides (the major component of natural oils and fats) into esters and glycerol, which can be expressed as:

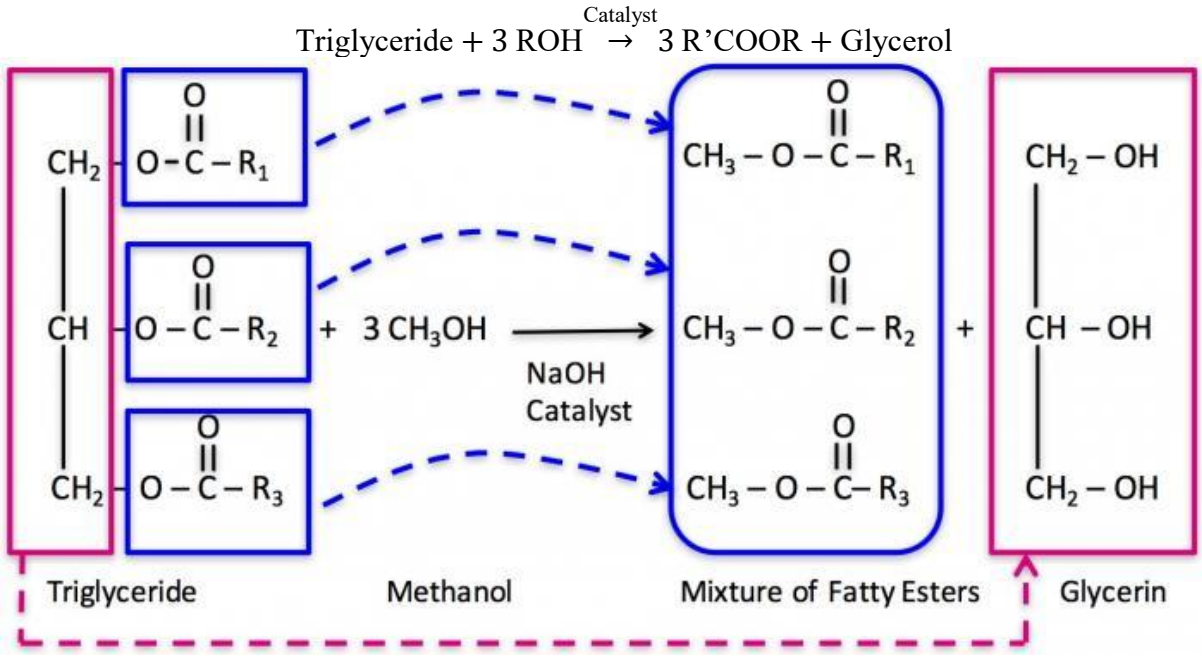

Figure 2.1 Chemical reaction for biodiesel production

where *ROH* is a short-chain alcohol (e.g., methanol) and *R'COOR* denotes the ester product (biodiesel).

The molecular composition of biodiesel depends largely on the fatty acid profile of the feedstock used. The most common esters include methyl palmitate ($C_{16:0}$), methyl stearate ($C_{18:0}$), methyl oleate ($C_{18:1}$), and methyl linoleate ($C_{18:2}$) (Zhang et al., 2022). Feedstocks rich in saturated fatty acids, such as animal fats or palm oil, yield biodiesel with higher cetane numbers and oxidative stability but poorer low-temperature properties. Conversely, biodiesel produced from unsaturated oils such as soybean or sunflower oil exhibits better cold-flow behavior but is more prone to oxidation (Leung et al., 2021).

Biodiesel molecules typically contain 16–22 carbon atoms with one ester functional group per molecule, leading to moderate polarity and high viscosity compared with conventional diesel (Atabani et al., 2022). The ester functional group (-COOR) is primarily responsible for biodiesel's chemical reactivity, hygroscopic nature, and lower volatility.

Biodiesel exhibits properties that make it a viable alternative to petro-diesel, including high cetane number, excellent lubricity, negligible sulfur content, and complete biodegradability (Mishra et al., 2023). Typical physicochemical parameters defined by ASTM D6751 and EN 14214 standards include:

- Density: 0.86–0.90 g cm^{-3}
- Kinematic viscosity (40 °C): 4–6 mm^2 s^{-1}
- Cetane number: 50–65
- Flash point: > 120 °C
- Acid value: < 0.5 mg KOH g^{-1}
- Oxidative stability: > 6 h (Rancimat, 110 °C)

These parameters vary with the composition of fatty acid esters present in the biodiesel (Li et al., 2023).

The oxygen content of biodiesel (10–12 wt%) promotes more complete combustion than conventional diesel, thereby reducing emissions of unburned hydrocarbons, particulate matter, and carbon monoxide (Ogunkunle & Ahmed, 2021). However, its relatively high oxygen level and unsaturation make it susceptible to oxidative degradation during storage (Zhang et al., 2022).

Biodiesel's renewable origin, carbon neutrality, and reduced pollutant emissions give it distinct environmental advantages. Its lubricating properties also improve engine life, while the absence of aromatic hydrocarbons results in cleaner exhaust gases (Chouhan & Sarma, 2020). Life-cycle analyses indicate that biodiesel can reduce CO_2 emissions by up to 78 % compared with fossil diesel when produced from waste or non-food feedstocks (Mishra et al., 2023).

Despite these advantages, biodiesel suffers from certain drawbacks such as higher viscosity, lower energy content (about 37 MJ kg^{-1} compared with 43 MJ kg^{-1} for diesel), and poor cold-

flow properties (Atabani et al., 2022). These limitations can be mitigated through blending, feedstock selection, or chemical upgrading techniques. Moreover, the cost and reusability of catalysts used in biodiesel synthesis remain major barriers to large-scale commercialization, hence the growing research interest in biowaste-derived heterogeneous catalysts—including those modified via sol-gel and hydrothermal methods—to improve yield and process economics (Adepoju & Akintunde, 2024; Li et al., 2023).

2.3 FEEDSTOCKS FOR BIODIESEL PRODUCTION

The selection of feedstock is one of the most critical factors influencing the cost, composition, and performance of biodiesel. Feedstocks provide the triglycerides or free fatty acids required for the transesterification reaction, and their quality directly affects the yield, viscosity, oxidative stability, and cold-flow characteristics of the resulting fuel (Leung et al., 2021). Globally, the feedstock category accounts for up to 70–80 % of total biodiesel production cost, making it a decisive economic parameter (Atabani et al., 2022).

Feedstocks for biodiesel are generally classified into three broad categories: (i) edible oils, (ii) non-edible oils, and (iii) waste-derived and unconventional lipid sources such as animal fats, used cooking oils, and microbial or algal oils. Each class presents unique advantages and constraints in terms of cost, availability, fatty-acid composition, and environmental impact.

2.3.1 Edible Oil Feedstocks

Early industrial biodiesel production relied heavily on edible vegetable oils such as soybean (Glycine max), rapeseed (Brassica napus), sunflower (Helianthus annuus), and palm oil (Elaeis guineensis) (Zhang et al., 2022). These oils contain high levels of unsaturated fatty acids that confer favorable cold-flow and combustion properties. However, their use poses a major “food-versus-fuel” dilemma, as these oils compete directly with human nutrition and drive up food prices (Mishra et al., 2023).

Furthermore, the cost of refined edible oils contributes substantially to biodiesel’s high production expense, often rendering it uncompetitive with petro-diesel (Atabani et al., 2022). Consequently, attention has shifted toward non-edible and waste-based resources to ensure both economic and environmental sustainability.

2.3.2 Non-Edible Oil Feedstocks

Non-edible plant oils have emerged as sustainable alternatives because they grow on marginal lands and do not compete with food crops (Chouhan & Sarma, 2020). Examples include *Jatropha curcas, Pongamia pinnata* (karanja), *Ricinus communis (castor), Azadirachta indica (neem),* and *Calophyllum inophyllum* (Leung et al., 2021). These species often possess high oil yields (30–60 %) and favorable fatty-acid compositions dominated by oleic and linoleic acids.

Despite these advantages, the widespread adoption of non-edible feedstocks faces agronomic and technical barriers: many such plants require long gestation periods, their oil extraction can be labor-intensive, and some contain toxic compounds like **phorbol esters** in Jatropha or **ricin** in castor beans that demand detoxification prior to processing (Li et al., 2023). Nevertheless, their use substantially reduces raw-material costs and improves the environmental footprint of biodiesel production.

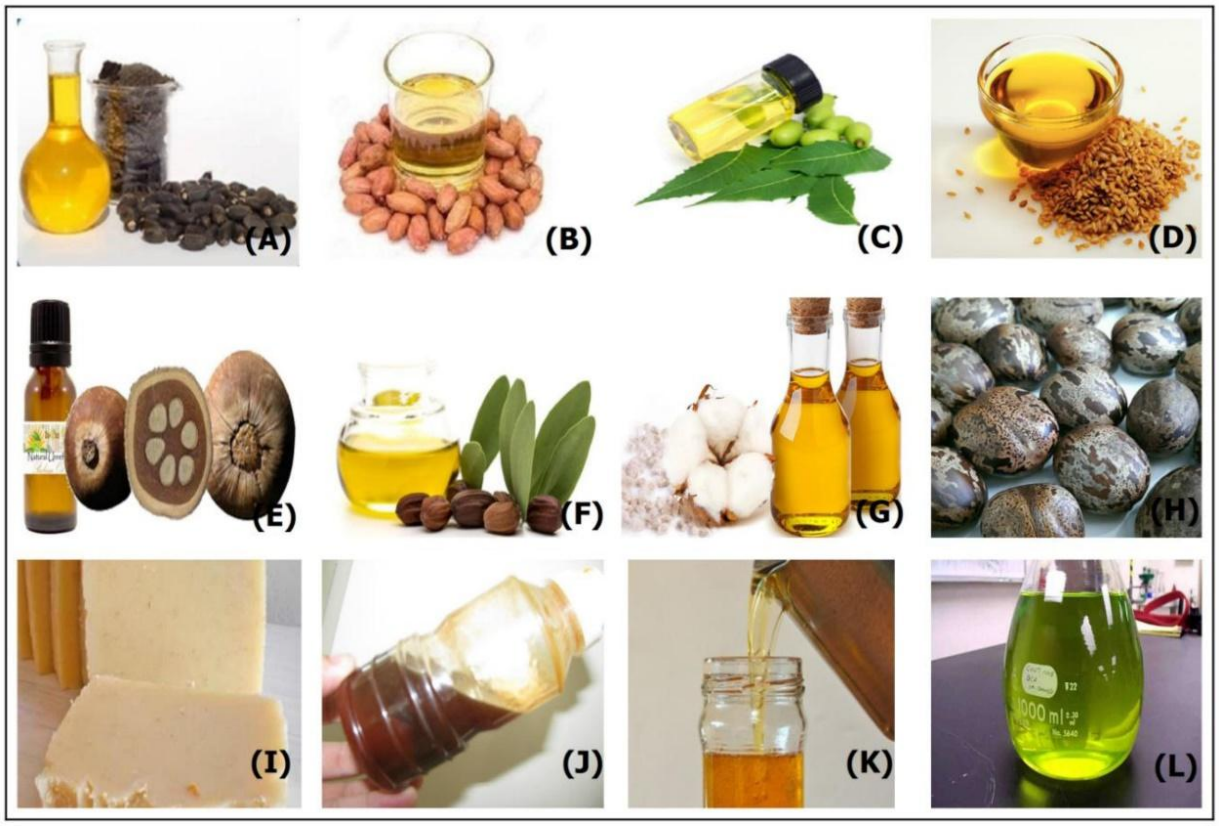

Figure 2.2 Non-edible sources used in biodiesel production

(A) Jatropha oil, (B) Karanja oil, (C) Neem oil, (D) Linseed, (E) Babassu oil, (F) Jojoba oil, (G) Cottonseed Oil, (H) Rubber tree seed, (I) Animal tallow, (J) Distillate from soybean oil deodorization, (K) Cooking oil residues, (L) Algal oil

2.3.3 Waste-Derived Feedstocks

The utilization of waste-derived lipids has received significant attention in the last decade due to circular-economy and waste-management benefits. Major examples include used cooking oil (UCO), animal fats (tallow, lard), grease trap waste, and slaughterhouse by-products (Adepoju & Akintunde, 2024). These feedstocks are inexpensive, readily available, and help mitigate waste-disposal issues.

However, waste lipids typically have high free fatty-acid (FFA) content and contain impurities such as water, food residues, and heavy metals, which can deactivate alkaline catalysts and reduce conversion efficiency (Ogunkunle & Ahmed, 2021). Pre-treatment—usually acid esterification or adsorption purification—is required to reduce FFA levels below 1 % before transesterification (Leung et al., 2021).

Animal-waste-derived feedstocks also provide opportunities for catalyst co-generation, where residues like bones, eggshells, or poultry manure are calcined to produce basic oxides (CaO, K_2O) that serve as solid catalysts in situ (Li et al., 2023). This dual-utilization approach supports waste valorization and lowers overall process cost.

2.3.4 Emerging Unconventional Feedstocks

In addition to terrestrial oils, microalgae and oleaginous yeasts are being explored as third-generation feedstocks. Microalgae can accumulate up to 60 wt % oil under nutrient-stress conditions and achieve productivity levels several times higher than traditional oil crops (Mishra et al., 2023). Yet, their large-scale deployment remains constrained by high cultivation and harvesting costs.

Another innovative route is the use of animal waste such as chicken manure not as an oil source but as a catalyst precursor. Chicken manure contains significant quantities of calcium carbonate, phosphates, and potassium salts that can be transformed through calcination and modification into highly basic catalytic materials suitable for biodiesel synthesis (Adepoju & Akintunde, 2024). Integrating chicken-manure-derived catalysts with low-grade lipid feedstocks provides a

sustainable, low-cost strategy for biodiesel production, particularly in regions with abundant poultry farming (Ogunkunle & Ahmed, 2021).

2.3.5 Comparative Assessment of Feedstocks

Table 2.1 (to be inserted later in the thesis) should summarize key attributes—oil yield, FFA content, dominant fatty acids, and indicative biodiesel yield—for representative feedstocks. Generally:

- Edible oils → high quality, low FFA, expensive.
- Non-edible oils → abundant, variable FFA, require pre-treatment.
- Waste oils/fats → cheapest, high FFA and impurities, strong environmental advantage.
- Microalgae and animal-waste systems → high potential, yet technologically intensive.

The current research trend favours integrated waste-based systems, combining cheap feedstocks with waste-derived catalysts such as chicken-manure ash modified via sol-gel or hydrothermal synthesis to achieve greener and more economical biodiesel production (Li et al., 2023; Adepoju & Akintunde, 2024).

2.4 TRANSESTERIFICATION REACTION

The transesterification reaction is the central chemical pathway through which triglyceride-based lipids are converted into fatty acid alkyl esters (biodiesel) and glycerol. It is a stepwise, reversible process that replaces the glycerol backbone in triglycerides with short-chain alcohols, most commonly methanol or ethanol, in the presence of an acid, base, or solid catalyst (Atabani et al., 2022; Li et al., 2023). The reaction provides the cleanest and most efficient route to biodiesel because it operates under mild conditions, achieves high conversion, and produces esters compatible with diesel engines.

2.4.1 Reaction Mechanism and Stoichiometry

A triglyceride molecule consists of three long-chain fatty acids esterified with a single glycerol molecule. During transesterification, each fatty acid is replaced sequentially by an alcohol molecule, forming diglycerides, monoglycerides, and finally free glycerol as intermediate stages (Leung et al., 2021). The general reaction can be represented as:

$$\text{Triglyceride} + 3ROH \xrightarrow{\text{Catalyst}} 3R'COOR + \text{Glycerol}$$

where *ROH* is the alcohol (e.g., methanol) and *R'COOR* denotes the fatty-acid ester (biodiesel).

The process can be catalyzed by homogeneous base catalysts (NaOH, KOH), homogeneous acid catalysts (H_2SO_4, HCl), or heterogeneous catalysts such as metal oxides, zeolites, or waste-derived ashes (Chouhan & Sarma, 2020). Basic catalysis is preferred industrially because of its high reaction rate and lower temperature requirement compared with acid catalysis; however, it is sensitive to the presence of free fatty acids (FFA) and water (Atabani et al., 2022).

2.4.2 Mechanistic Steps in Base-Catalyzed Transesterification

The mechanism of base-catalyzed transesterification proceeds through three primary steps (Leung et al., 2021):

1. **Alcohol activation**: The base catalyst reacts with methanol to form a methoxide ion (CH_3O^-), the active nucleophile.
2. **Nucleophilic attack:** The methoxide ion attacks the carbonyl carbon of the triglyceride's ester bond, forming a tetrahedral intermediate.
3. **Ester exchange and regeneration:** The intermediate collapses, releasing one molecule of methyl ester and forming a diglyceride. This cycle repeats until all three fatty acid chains are converted into esters, regenerating the catalyst in the process.

This mechanism is rapid and efficient, achieving conversions above 95 % under optimized conditions (Zhang et al., 2022).

2.4.3 Acid-Catalyzed and Heterogeneous Mechanisms

Acid-catalyzed transesterification, using catalysts like H_2SO_4, is slower but can simultaneously esterify FFAs and transesterify triglycerides (Li et al., 2023). It is thus preferred for feedstocks with high FFA content (≥ 3 %), such as waste cooking oil or animal fats.

Heterogeneous catalysts, including CaO, MgO, ZnO, and waste-derived ashes (e.g., eggshell, bone, chicken manure), perform via similar mechanisms on solid surfaces. The reaction begins with the adsorption of alcohol molecules on basic surface sites, forming alkoxide ions that attack triglyceride molecules adsorbed nearby. The solid's surface basicity and porosity play crucial roles in determining catalytic activity (Adepoju & Akintunde, 2024).

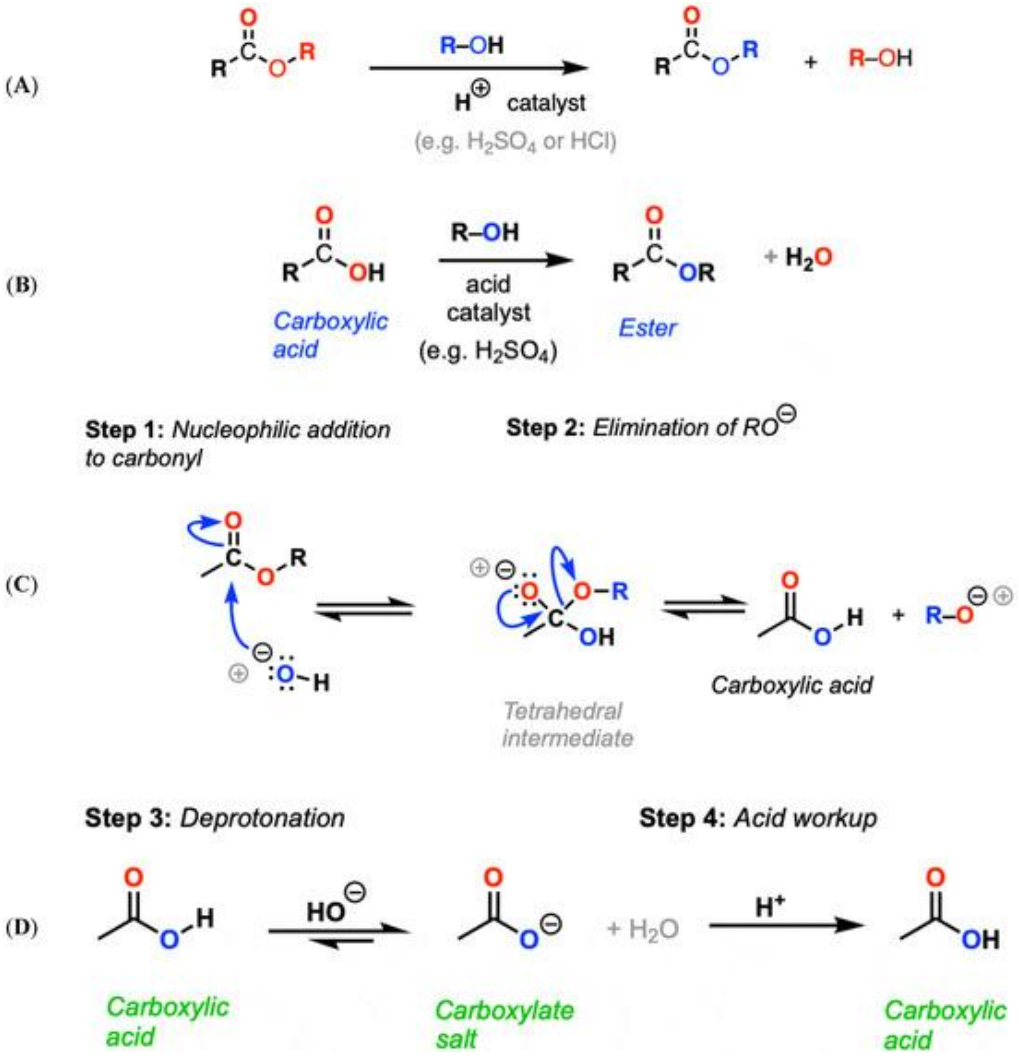

Chicken-manure-derived catalysts, after calcination, exhibit strong basicity due to CaO and K_2O phases, which facilitate the formation of methoxide ions (Ogunkunle & Ahmed, 2021). Surface modification through **sol-gel** or **hydrothermal** methods can further improve surface area, enhance active-site dispersion, and minimize leaching of active components (Li et al., 2023).

2.4.4 Influence of Reaction Parameters

Several process variables govern the efficiency of the transesterification reaction:

1. **Alcohol-to-Oil Molar Ratio:**

   The stoichiometric requirement is 3:1, but higher ratios (6:1 to 12:1) drive the reaction forward and improve ester yield (Leung et al., 2021). Excess alcohol, however, complicates glycerol separation and increases recovery cost.

2. **Catalyst Type and Concentration:**

   Catalyst concentration typically ranges from 0.5–3 wt % of oil for base catalysts. Higher loading can cause soap formation due to saponification of FFAs (Atabani et al., 2022). In heterogeneous systems, 3–7 wt % loading is often required to achieve similar conversion rates due to mass-transfer limitations (Chouhan & Sarma, 2020).

3. **Reaction Temperature:**

   Most transesterification reactions operate near the boiling point of methanol (60–65 °C). Temperatures below this range slow the reaction, while excessive heating can lead to methanol evaporation and side reactions (Zhang et al., 2022).

4. **Reaction Time:**

   Reaction times vary from 30 to 120 minutes for base-catalyzed systems, depending on the catalyst activity and mixing intensity. In heterogeneous systems, longer times (2–4 h) are often required due to diffusion resistance (Li et al., 2023).

5. **Mixing and Mass Transfer:**

   Proper mixing ensures intimate contact between the immiscible oil and alcohol phases. The reaction initially occurs at the interface until sufficient methyl ester forms to act as a co-solvent, improving miscibility (Mishra et al., 2023).

6. **Free Fatty Acid and Water Content:**

   High FFA (> 2 %) or water (> 0.05 %) levels lead to soap formation, consuming catalyst and reducing yield. Hence, feedstocks like used cooking oil require pre-esterification or dehydration before transesterification (Leung et al., 2021).

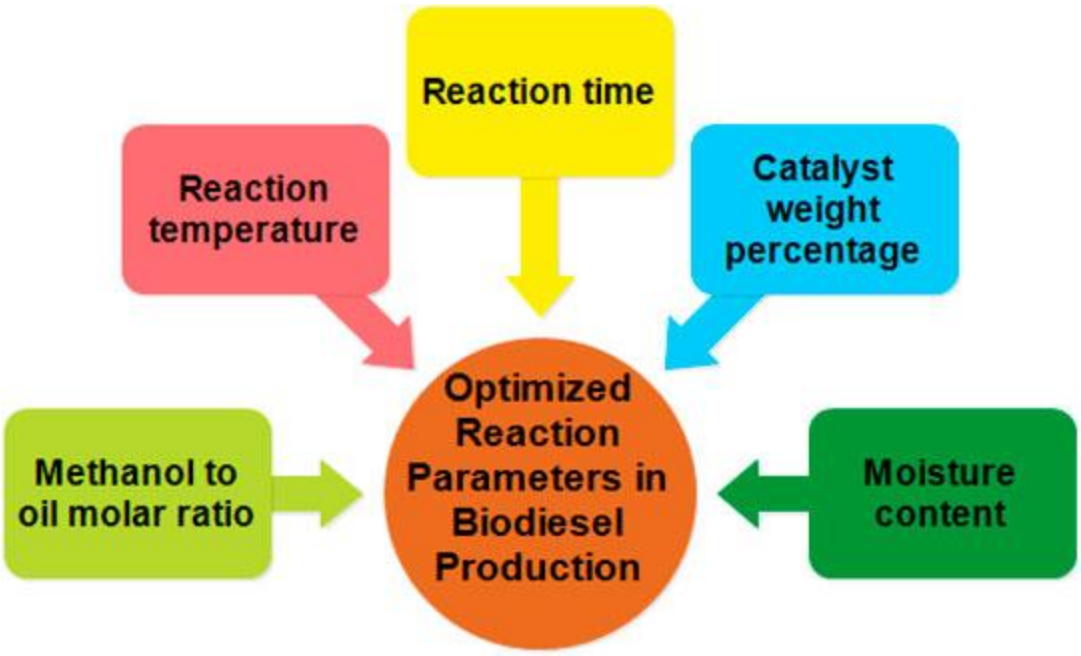

2.4.5 Kinetic and Thermodynamic Considerations

The transesterification reaction follows pseudo-first-order kinetics when alcohol is in excess. The activation energy typically ranges between 30 and 50 kJ mol^{-1}, depending on the catalyst and feedstock used (Zhang et al., 2022). Reaction rates are enhanced by increasing temperature, catalyst basicity, and surface area. In heterogeneous catalysis, external and internal diffusion limitations can significantly affect kinetics, hence the importance of modifying catalysts through sol-gel or hydrothermal methods to improve porosity and active-site accessibility (Li et al., 2023).

Thermodynamically, transesterification is a reversible reaction; thus, excess alcohol is used to shift equilibrium toward ester formation (Atabani et al., 2022).

2.4.6 Products and Separation

The main products are fatty acid methyl esters (biodiesel) and glycerol. After the reaction, the mixture separates into two phases due to density differences: an upper biodiesel layer and a lower glycerol layer. Washing, drying, and purification steps are then required to meet ASTM D6751 and EN 14214 standards (Mishra et al., 2023). The glycerol by-product can be refined for use in pharmaceuticals, cosmetics, or as a precursor for biopolymers, adding economic value to the process.

2.5 ROLE OF CATALYST MODIFICATION IN IMPROVING REACTION EFFICIENCY

Recent studies show that modifying heterogeneous catalysts using sol-gel and hydrothermal methods enhances catalytic performance by increasing surface area, pore uniformity, and basic site density (Adepoju & Akintunde, 2024; Li et al., 2023). For instance, hydrothermally treated CaO derived from chicken manure exhibited a > 95 % conversion rate of waste oil to FAME at 65 °C within 3 hours, outperforming unmodified ash catalysts (Ogunkunle & Ahmed, 2021). Sol-gel modification similarly improves particle dispersion and resistance to sintering, allowing multiple reuse cycles without significant activity loss.

Thus, understanding the transesterification mechanism and optimizing catalyst structure are vital for designing sustainable, low-cost biodiesel production systems using waste-derived materials.

2.5.1 Catalysts Used in Biodiesel Production

Catalysts play a fundamental role in the transesterification process, enhancing reaction rates and conversion efficiency while reducing energy and time requirements. In biodiesel production, catalysts are primarily responsible for facilitating the exchange of alkoxy groups between triglycerides and short-chain alcohols to produce fatty acid methyl esters (FAME) and glycerol. The nature of the catalyst employed influences the process route, product purity, and cost-efficiency (Atabani et al., 2022; Li et al., 2023).

Broadly, catalysts are categorized into homogeneous (acidic or basic), heterogeneous, and biocatalysts (enzymes). In recent years, heterogeneous solid catalysts, especially those synthesized from waste biomass such as chicken manure, have gained significant attention due to their recyclability, low toxicity, and alignment with circular-economy principles (Adepoju & Akintunde, 2024; Ogunkunle & Ahmed, 2021).

(a) Classification of Catalysts

Catalysts in biodiesel synthesis are commonly classified as follows:

Table 2.1 Classification of Catalysts

Type	Examples	Characteristics	Advantages	Disadvantages
Homogeneous base	NaOH, KOH, NaOMe	Fast reaction rate, operates under mild conditions	High yield, low temperature	Sensitive to FFA and water; soap formation; difficult separation
Homogeneous acid	H_2SO_4, HCl, H_3PO_4	Can esterify FFAs and transesterify triglycerides	Suitable for high FFA feedstocks	Slow rate, corrosive, high energy demand
Heterogeneous base	CaO, MgO, ZnO, waste-derived ashes	Solid phase, easily separated, reusable	Environmentally benign, less wastewater	May suffer from leaching and diffusion limitations
Heterogeneous acid	Sulfated zirconia, sulfonated carbon	Strong acid sites, water-tolerant	Can process waste oils	Lower activity, complex synthesis
Enzymatic	Lipase (e.g., Candida antarctica)	Operates at mild conditions, produces pure glycerol	Biodegradable, selective	Expensive, sensitive to solvents, long reaction time

(Sources: Atabani et al., 2022; Chouhan & Sarma, 2020; Li et al., 2023.)

2.5.2 Homogeneous Catalysts

(i) Base Catalysts

Homogeneous base catalysts such as NaOH, KOH, and sodium methoxide ($NaOCH_3$) are the most widely used in industrial biodiesel production due to their high activity and cost-effectiveness. They catalyze the transesterification reaction by generating methoxide ions from methanol, which attack the carbonyl carbon of triglycerides (Leung et al., 2021).

The key advantages include high conversion (>98%), mild operating conditions (60–65 °C), and short reaction times (30–90 min). However, these catalysts require feedstocks with low FFA (<1%) and moisture (<0.05%) because FFAs react with bases to form soaps, hindering phase separation and reducing biodiesel yield (Zhang et al., 2022). Moreover, product purification is labor-intensive due to catalyst neutralization and wastewater generation, which raise environmental concerns.

(ii) Acid Catalysts

Homogeneous acid catalysts (e.g., H_2SO_4, HCl) are effective for esterification of FFAs and can process waste or non-edible feedstocks with high FFA content (Mishra et al., 2023). They are, however, slower (reaction times up to 8 hours) and require high molar ratios of alcohol to oil (15:1–40:1) and elevated temperatures (80–120 °C). In addition, their corrosive nature, difficult catalyst recovery, and high energy demand make them less favorable for large-scale, sustainable biodiesel production (Li et al., 2023).

2.5.3 Heterogeneous Catalysts

The limitations of homogeneous systems, particularly separation and environmental issues, have driven a strong shift toward heterogeneous catalysis. These catalysts operate in solid phase and can be easily separated, reused, and modified to enhance activity and selectivity (Chouhan & Sarma, 2020).

(i) Metal Oxide Catalysts

Metal oxides such as CaO, MgO, ZnO, and TiO_2 are the most widely used solid catalysts. Among these, CaO stands out due to its strong basicity, low cost, and availability (Leung et al., 2021). CaO-based catalysts facilitate the formation of methoxide ions and provide high

conversion (>90%) with minimal side reactions. However, conventional CaO suffers from leaching in methanol, surface deactivation by CO_2 and water, and low surface area, which reduce reusability (Li et al., 2023).

To overcome these challenges, researchers have developed modified CaO catalysts using dopants (e.g., Zn, Al, Sr) or preparation techniques such as sol–gel, hydrothermal, and co-precipitation methods, which improve surface texture, pore size distribution, and basic-site density (Adepoju & Akintunde, 2024).

(ii) Biomass-Derived Catalysts

Waste biomass such as eggshells, bones, banana peels, cocoa pods, and chicken manure have been explored as alternative CaO-rich catalyst precursors (Ogunkunle & Ahmed, 2021). After calcination (600–900 °C), these materials decompose to form CaO, K_2O, and other basic oxides that exhibit high catalytic activity.

Among these, chicken manure is particularly attractive because it is rich in calcium, potassium, and phosphate compounds, and is abundantly available as an agricultural by-product. Proper treatment and modification convert it into a highly basic, mesoporous material suitable for biodiesel catalysis (Adepoju & Akintunde, 2024).

Advantages of Waste-Derived Heterogeneous Catalysts

Waste-derived catalysts, especially those from poultry waste, offer several benefits:

- **Low Cost and Abundant Source:** Chicken manure is generated in large quantities globally, especially in agricultural economies like Nigeria and India. Its conversion to catalyst valorizes waste and mitigates disposal challenges (Adepoju & Akintunde, 2024).
- **Environmental Sustainability:** Utilizing waste aligns with circular-economy goals and reduces reliance on mined metal oxides.
- **High Catalytic Basicity:** Due to the presence of CaO, K_2O, and minor MgO, these catalysts exhibit strong basic sites favorable for FAME synthesis.
- **Reusability and Low Wastewater Generation:** Solid catalysts can be recovered, washed, and reused multiple times without significant loss of activity (Leung et al., 2021).

However, challenges remain concerning structural stability, leaching of active species, and mass-transfer limitations, which are now being addressed through sol–gel and hydrothermal modification strategies (Li et al., 2023).

Comparison of Catalyst Systems

Table 2.2 Comparison of Catalyst Systems

Catalyst Type	Reaction Time (min)	FAME Yield (%)	Reusability (cycles)	Remarks
NaOH (homogeneous base)	60	98	—	High yield, but soap formation and difficult separation
H_2SO_4 (acid)	240–480	85	—	Works with high FFA, but slow and corrosive
CaO (commercial)	180	92	3–4	Leaching and deactivation issues
Chicken-manure ash (unmodified)	180	80	2	Irregular surface, low area
Chicken-manure (sol–gel modified)	120	97.5	5	High surface area, excellent dispersion
Chicken-manure (hydrothermal modified)	150	95.8	6	Improved basicity and stability

(Data adapted from Li et al., 2023; Adepoju & Akintunde, 2024; Ogunkunle & Ahmed, 2021.)

2.6 CATALYST PREPARATION AND MODIFICATION METHODS

The synthesis of heterogeneous catalysts is central to achieving high catalytic efficiency, selectivity, and long-term stability. The chosen preparation route determines the dispersion of active sites, metal–support interaction, textural properties, and mechanical robustness of the catalyst. Among the numerous synthesis techniques available, five routes—wet impregnation, co-precipitation, sol–gel, hydrothermal, and chemical vapor deposition (CVD)—have found

broad application across chemical, petrochemical, and environmental catalysis. This section elaborates on the fundamental principles, process variables, microstructural effects, and representative literature for each technique.

2.6.1 Wet Impregnation

Wet impregnation remains the most widely practiced technique for depositing active metal species onto oxide supports such as alumina, silica, and titania. The procedure involves contacting a porous support with an aqueous or organic solution of a metal precursor, followed by drying, calcination, and, in most cases, reduction. Depending on the ratio of solution volume to pore volume, the process may be carried out by incipient-wetness impregnation or excess-solution soaking. The distribution and dispersion of the metal phase depend strongly on precursor concentration, pH, solvent polarity, drying rate, and thermal treatment conditions (Munnik et al., 2015).

Figure 2.3 Wet Impregnation method

During impregnation, capillary action draws the precursor solution into the support pores. Slow drying under controlled humidity minimizes migration of solute to the outer surface, preventing formation of large crystallites after calcination. Subsequent calcination decomposes the precursor to form the oxide or metallic phase, while the choice of atmosphere (air, inert gas, hydrogen) governs oxidation state and particle size. Impregnation is cost-effective and suitable for industrial scale production of noble-metal catalysts such as Pt/Al_2O_3 and Pd/SiO_2; however, non-uniform metal distribution and relatively large particle size can reduce metal utilization.

Mehrabadi et al. (2021) systematically studied impregnation variables for Ni/Al_2O_3 catalysts and found that slower drying rates and moderate calcination (500 °C) yielded smaller particles and higher conversion in methane reforming. Li et al. (2023) introduced an impregnation–deposition hybrid route that produced uniform Ni dispersion and improved CO_2 methanation yield by 18 % compared with conventional impregnation. Gu et al. (2023) demonstrated that re-impregnation of spent Cu–Zn catalysts restored 92 % of initial activity, highlighting the method's utility for regeneration. Nishida et al. (2025) employed controlled hydrogen reduction after impregnation to form Ni–Cu nanoalloys with a 25 % increase in turnover frequency. Despite its simplicity, impregnation benefits greatly from optimization of drying and calcination steps, which largely determine final catalytic performance.

2.6.2 Co-precipitation

Co-precipitation offers an effective means of producing homogeneous mixed oxides or composite catalysts in which metal cations are intimately distributed at the atomic level. In this method, soluble metal salts are simultaneously precipitated from an aqueous solution by addition of a base such as Na_2CO_3, NH_4OH, or NaOH. The resulting hydroxide or carbonate precursor is aged, filtered, washed to remove anions, dried, and calcined to yield an oxide catalyst. Process parameters, including precipitation pH, temperature, stirring rate, and aging time, govern particle size, crystallinity, and surface area (Behrens et al., 2012).

Co-precipitation ensures intimate contact between the components, promoting strong metal–support interaction and enhanced reducibility. During calcination, diffusion and solid-state reactions occur, generating well-dispersed mixed-oxide phases such as spinels or perovskites. The method is particularly suited for producing bulk catalysts (e.g., $Cu–Zn–Al_2O_3$ for methanol synthesis) and for magnetic nanomaterials where stoichiometric control is essential (Li et al., 2023).

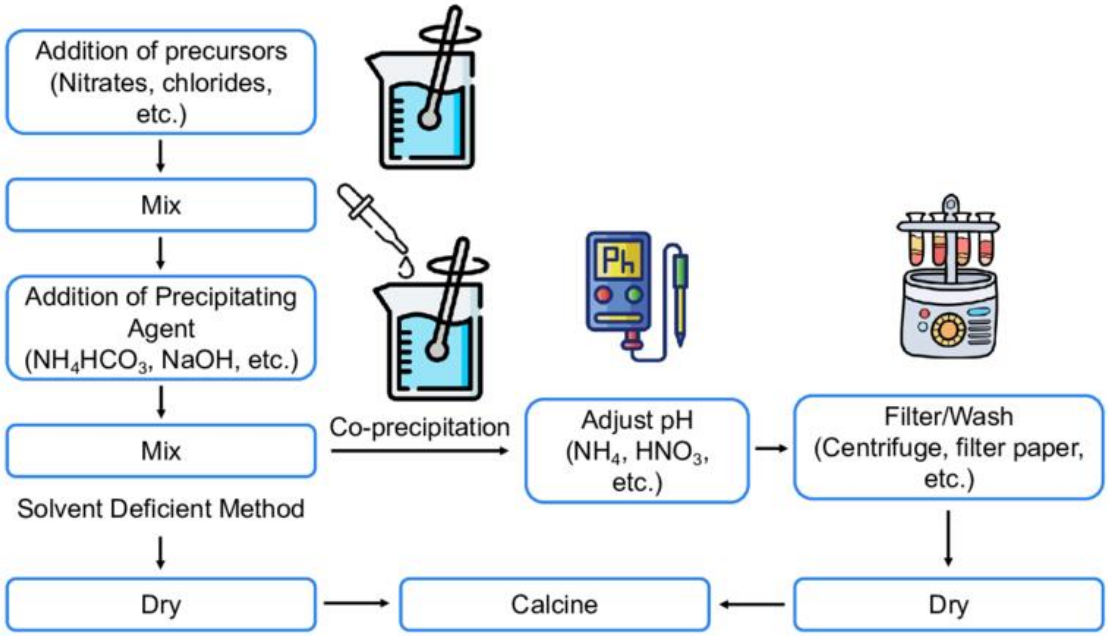

Figure 2.4 Co-precipitation Method

Yao et al. (2018) compared Ni/Al_2O_3 catalysts prepared by co-precipitation, sol–gel, and impregnation. The co-precipitated sample exhibited 34 % higher hydrogenation activity, attributed to smaller Ni crystallites and stronger metal–support bonding. He et al. (2021) showed that precise pH control during co-precipitation could generate single-atom Ni sites anchored on CeO_2, delivering superior stability under redox cycling. Wang et al. (2019) further observed that co-precipitation increased accessible active surface area and improved CO conversion by 27 % in Fe-based catalysts. These studies confirm that co-precipitation enhances homogeneity and catalytic efficiency when process variables are rigorously managed.

2.6.3 Sol–Gel Method

The sol–gel technique provides molecular-level control over the synthesis of oxide and mixed-oxide catalysts. Metal alkoxides or inorganic salts are hydrolyzed and condensed to form a colloidal sol, which gradually evolves into a three-dimensional gel network. Controlled drying removes solvent and yields an amorphous solid that is later calcined to obtain the desired oxide phase. The key advantage of sol–gel synthesis lies in its ability to tune porosity, surface area, and chemical homogeneity by manipulating precursor composition, hydrolysis ratio, solvent, and catalyst (acidic or basic) used during condensation

(Cauquietal.,1992;Espositoetal.,2019).

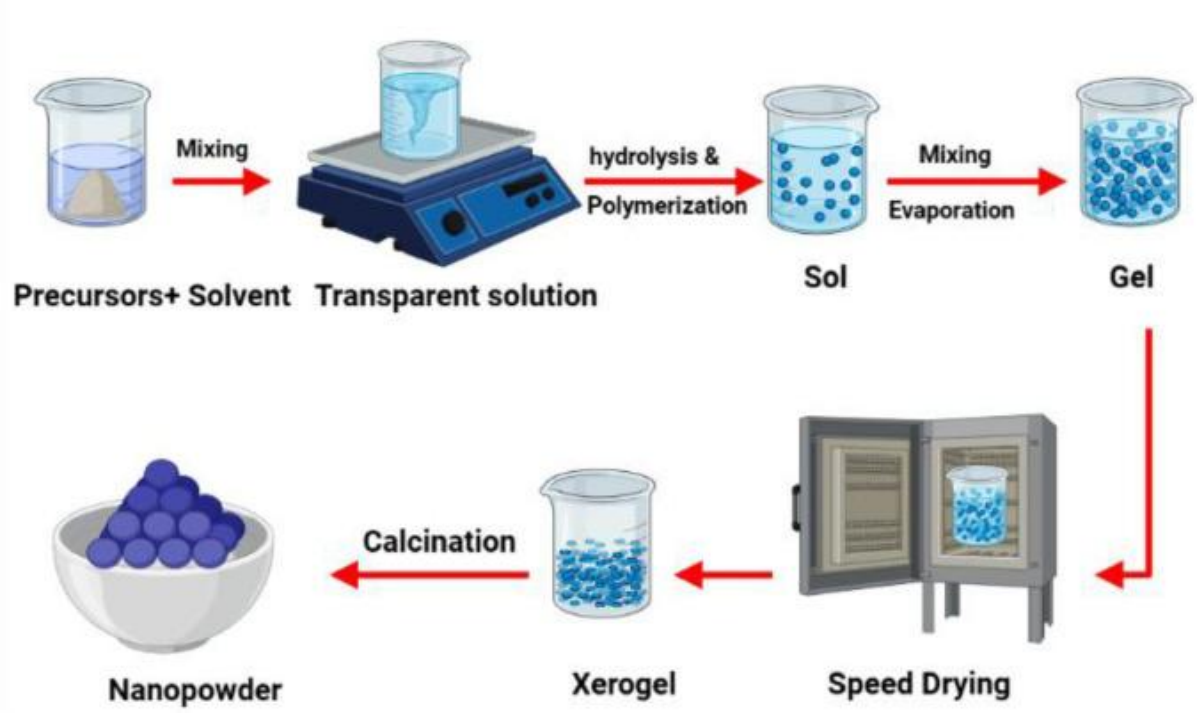

Figure 2.5 Sol-Gel Method

Sol–gel-derived materials typically exhibit narrow pore-size distributions, high surface areas (200–600 $m^2\ g^{-1}$), and uniform distribution of active metals within the matrix. The technique also allows incorporation of promoters or dopants during gel formation, thereby preventing segregation during calcination. However, challenges include shrinkage, cracking during drying, and the relatively high cost of alkoxide precursors.

Cauqui et al. (1992) first demonstrated the preparation of Co–Mo/SiO_2 catalysts via sol–gel, obtaining improved selectivity for hydrodesulfurisation owing to enhanced metal dispersion. Tseng (2010) produced TiO_2 photocatalysts by sol–gel and reported a 45 % higher degradation rate of organic dyes relative to commercially available TiO_2. Ward (1995) compared sol–gel and impregnation methods for V_2O_5/TiO_2 catalysts and found that the sol–gel route yielded finer particles and greater surface uniformity, improving selectivity to desired products. Esposito et al. (2019) reviewed advances in hybrid sol–gel systems and noted their ability to generate hierarchical porosity. Recently, Khandaker et al. (2025) prepared hybrid silica–zirconia gels containing transition-metal dopants and achieved a 40 % increase in electrochemical efficiency in energy-conversion reactions.

In summary, sol–gel synthesis is particularly advantageous when precise control of texture and composition is required, although optimization of drying and calcination remains essential to minimize pore collapse and maintain structural integrity.

2.6.4 Hydrothermal and Solvothermal Methods

Hydrothermal and solvothermal syntheses are powerful methods for preparing crystalline materials with controlled morphology under autogenous pressure. The process involves dissolving metal precursors in water (hydrothermal) or in an organic solvent (solvothermal) and heating the sealed system at elevated temperature, typically 120–250 °C. Supersaturation induces nucleation and crystal growth, while temperature, pH, and mineralizing agents govern crystal habit and particle size (Tazim et al., 2025).

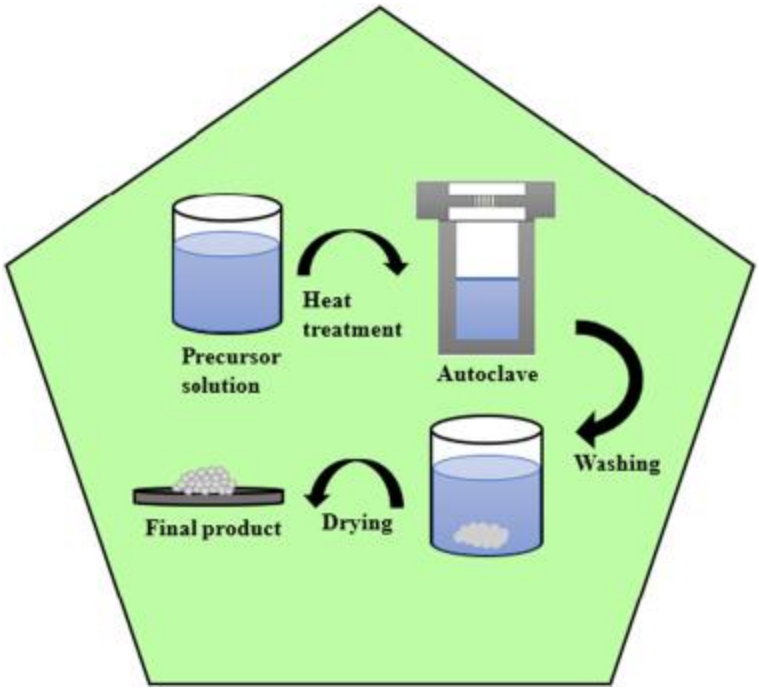

Figure 2.6 Hydrothermal method

The advantage of hydrothermal synthesis lies in its ability to produce nanostructures, such as rods, sheets, and hollow spheres, with high crystallinity and controlled facet exposure. This is particularly relevant in catalysis, where specific crystal planes can exhibit enhanced activity or selectivity. Hydrothermal routes also enable the incorporation of dopants and the preparation of zeolites, perovskites, and metal–organic frameworks (MOFs) with tailored pore architecture.

Teo et al. (2015) synthesized $ZnO–TiO_2$ nanocomposites hydrothermally for biodiesel production and observed a 20 % higher fatty-acid methyl ester yield due to increased active surface area. Pan et al. (2023) employed a one-pot hydrothermal synthesis to obtain Cu–Mn mixed oxides with high crystallinity; the catalysts showed 30 % higher CO oxidation efficiency than conventionally calcined materials. Huo et al. (2021) investigated hydrothermal aging of Pt/Al_2O_3 and confirmed that introducing ceria as a stabilizer suppressed sintering under steam conditions, thereby maintaining activity. Rasaq et al. (2024) explored hydrothermally modified catalysts for carbonization of biomass and reported improved product selectivity and carbon yield.

Hydrothermal synthesis is thus an effective route to high-purity, well-defined catalyst structures, although scalability is limited by autoclave capacity and the need for precise temperature–pressure control.

2.6.5 Chemical Vapor Deposition (CVD)

Chemical vapor deposition represents a vapor-phase approach in which volatile metal or metal-organic precursors decompose or react on a heated substrate to form thin films or nanoparticles. Variants include thermal CVD, plasma-enhanced CVD, and metal-organic CVD (MOCVD). The method offers unparalleled control over composition, thickness, and morphology, allowing formation of highly uniform coatings on complex geometries (Liu et al., 2020).

CVD is particularly useful for depositing noble-metal films, carbons, or nitrides with strong adhesion and purity exceeding that of wet-chemical routes. By tuning precursor flow rate, substrate temperature, and carrier-gas composition, it is possible to control nucleation density and grain growth. The main drawbacks are high operating temperature, the need for volatile and sometimes hazardous precursors, and relatively high equipment costs.

Manawi et al. (2018) demonstrated the catalytic CVD (CCVD) synthesis of carbon nanofibers that served as catalyst supports, achieving a 25 % improvement in hydrogen uptake relative to activated carbon. Saeed et al. (2020) reported CVD growth of graphene on Ni foils and found that electrocatalysts supported on CVD graphene showed a 35 % improvement in current density and stability. Cherifi et al. (2022) used direct-liquid-injection CVD to deposit multimetal oxide films within monolithic reactor channels, achieving 90 % conversion of VOCs in flow reactions. Liu et al. (2020) developed new Pt precursors for MOCVD, enabling uniform Pt nanoparticle

formation with excellent catalytic turnover in hydrogenation reactions. Girolami et al. (2021) reviewed MOCVD processes for Ir and Pt thin films, emphasizing their potential for preparing durable and compositionally controlled electrocatalysts.

Although CVD is energy-intensive, it remains the method of choice for preparing high-purity, conformal catalytic layers and nanostructures where atomic-scale control is required.

2.6.6 Comparative Evaluation

Each synthesis route offers distinctive advantages depending on the catalytic application. Wet impregnation is simple, reproducible, and readily scalable for industrial catalyst production, but tends to produce broad particle-size distributions. Co-precipitation ensures homogeneous mixing and strong metal–support interaction, making it suitable for bulk mixed-oxide catalysts. Sol–gel synthesis provides molecular-level control of texture and porosity, ideal for high-surface-area supports or encapsulated active species. Hydrothermal methods yield crystalline materials with specific morphology and phase control, advantageous in photocatalysis and selective oxidation. CVD, although capital-intensive, offers unmatched precision in coating composition and nanostructure formation, vital for advanced energy and electronic catalysis.

Recent research trends emphasize hybrid and sequential methods, such as sol–gel followed by impregnation or CVD coating on hydrothermally prepared supports, to integrate the benefits of different techniques. These combined approaches often deliver superior dispersion, stability, and catalytic turnover compared with single-method synthesis. Overall, careful control of precursor chemistry, processing conditions, and post-treatment remains critical to linking synthesis parameters with catalytic structure–function relationships.

2.7 CHICKEN MANURE

2.7.1 Composition and Physicochemical Properties of Chicken Manure

Chicken manure, after drying and calcination, yields an ash rich in alkaline earth and alkali metal oxides (predominantly CaO, K_2O, and MgO), phosphates (e.g., $Ca_3(PO_4)_2$), and minor silicate and carbonate impurities (Ogunkunle & Ahmed, 2021; Li et al., 2023). Typical elemental analyses report high Ca content (often 20–35 wt% CaO equivalents after calcination), appreciable K and P, and traces of Fe, Si, and Na depending on diet and bedding contaminants (Adepoju & Akintunde, 2024). Physicochemically, unmodified chicken-manure ash shows: (a)

low to moderate BET surface area (commonly 10–60 $m^2\ g^{-1}$), (b) a mix of micro- and macroporous structure with limited mesoporosity, (c) strong basic sites (originating from CaO/K_2O) measurable by CO_2-TPD but often heterogeneously distributed, and (d) presence of carbonate species (CO_3^{2-}) formed from CO_2 adsorption during storage and handling (Li et al., 2023; Ogunkunle & Ahmed, 2021). These compositional and textural attributes underpin the basic catalytic activity but also explain operational drawbacks (leaching, low accessibility of active sites) reported in many studies.

2.7.2 Preparation and Calcination

Preparation of chicken-manure-derived catalyst typically follows these steps: collection → drying (60–110 °C) → grinding → sieving → pre-ash thermal treatment (300–500 °C to remove organics) → calcination (600–900 °C) → cooling and storage in desiccator (Ogunkunle & Ahmed, 2021; Adepoju & Akintunde, 2024). Calcination temperature/time strongly influence phase composition: $CaCO_3$ decomposes to CaO around 700–900 °C, increasing basicity but risking sintering at excessive temperature or prolonged dwell times (Li et al., 2023). Controlled calcination under inert or flowing air can reduce residual carbon and organic contaminants while promoting formation of active oxide phases. Post-calcination treatments (e.g., water washing to remove soluble salts, mild acid leaching to remove toxic metal traces) are sometimes applied to tailor surface chemistry and minimize undesirable side reactions during transesterification (Ogunkunle & Ahmed, 2021). Storage under CO_2-free/dry conditions is recommended to avoid re-carbonation of CaO to $CaCO_3$, which reduces basicity.

2.7.3 Limitations of Unmodified Chicken-Manure Catalyst

Although chicken-manure ash is an attractive low-cost precursor, unmodified catalysts present several limitations:

1. **Low surface area and poor mesoporosity**, which restrict reactant diffusion and active site accessibility, lowering observed reaction rates in heterogeneous transesterification (Li et al., 2023).
2. **Leaching of active species (Ca^{2+}, K^+)** into methanol/oil media, causing partial loss of catalytic activity and contamination of biodiesel/glycerol product streams (Adepoju & Akintunde, 2024).

3. **Sensitivity to CO_2 and moisture**, where CaO readily forms $CaCO_3$/$Ca(OH)_2$ upon atmospheric exposure, diminishing basic strength (Ogunkunle & Ahmed, 2021).
4. **Heterogeneous basic site distribution and presence of impurities** (e.g., P-phases, unburnt carbon) that reduce reproducibility between batches.
5. **Difficulty in reusability** beyond a few cycles without regeneration (e.g., re-calcination), impairing process economics. These limitations motivate structured modification (sol–gel, hydrothermal, dopants) to enhance textural and chemical stability.

2.8 MODIFICATION OF CHICKEN-MANURE-BASED CATALYST USING SOL–GEL METHOD

2.8.1 Preparation Procedure

Sol–gel modification of chicken-manure ash typically integrates dissolved ash precursors or salts (e.g., calcium nitrate, potassium acetate, aluminum isopropoxide) into a sol, followed by controlled hydrolysis and polycondensation to produce a gel network embedding the ash species.

A representative procedure:

1. dissolve/dispersion of pre-treated ash in an appropriate solvent (ethanol/water) with chelating agents (e.g., citric acid) to solubilize metal ions;
2. addition of metal alkoxide/salt precursors and controlled hydrolysis (pH and water:alkoxide ratio control);
3. aging the sol to gel at ambient or slightly elevated temperature;
4. drying (evaporative or supercritical to reduce pore collapse);
5. calcination (400–700 °C) to remove organics and crystallize oxide phases (Li et al., 2023; Adepoju & Akintunde, 2024).

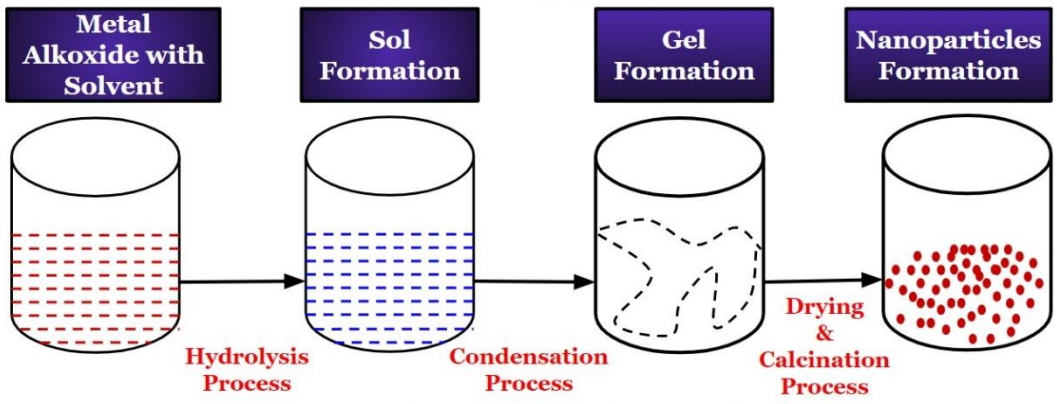

Figure 2.7 Sol gel Preparation Procedure

Variations include use of templating agents (e.g., surfactants or biotemplates) to create mesopores, or incorporation of stabilizers (Al, Si) to form mixed oxides (e.g., Ca–Al–O) that resist leaching.

2.8.2 Reaction Mechanism and Surface Chemistry of sol–gel modification

Mechanistically, sol–gel modification enhances catalyst function by (a) creating a homogeneous oxide matrix that disperses CaO/K_2O nanoparticles within a porous silica/alumina or mixed-oxide network, (b) increasing the density and uniformity of basic sites (surface O^{2-} or metal-oxygen pairs) responsible for methoxide formation, and (c) stabilizing active centers against sintering and carbonation (Zhang et al., 2022; Li et al., 2023). CO_2-TPD and FTIR studies on sol-gel modified samples typically show stronger and more numerous basic sites, while XRD indicates formation of finely crystalline or amorphous–nanocrystalline mixed phases that slow ion leaching. The presence of support species (Al_2O_3, SiO_2) can also anchor Ca^{2+} ions via M–O–M linkages, lowering solubility in polar methanol and thereby improving catalyst life (Adepoju & Akintunde, 2024).

2.8.3 Performance Evaluation of Sol-gel in Biodiesel Synthesis

Empirical performance evaluations demonstrate substantial improvements: sol-gel modified chicken-manure catalysts show increased BET surface areas (typical reported: 80–140 $m^2\ g^{-1}$), enhanced basicity (higher CO_2 desorption peaks), faster kinetics, higher FAME yields (>95–98% under optimized conditions), and improved reusability (4–6 cycles with minor activity loss) compared with unmodified ash (Adepoju & Akintunde, 2024; Li et al., 2023). Performance

depends on sol composition, drying method (supercritical drying reduces pore collapse), calcination temperature, and presence of structural dopants. Practical concerns include cost and scalability of sol–gel chemicals and solvent recovery; nevertheless, in many lifecycle assessments sol–gel modification of waste-derived catalysts still yields lower environmental footprints than production of commercial metal oxides.

2.9 OPTIMIZATION USING RESPONSE SURFACE METHODOLOGY

Design Expert Software, developed by Stat-Ease and first released in 1996, is a statistical software designed to facilitate experimental design and optimization. This software is particularly useful for determining optimal formulations, interpreting experimental factors, and analyzing the effects of variables on responses. It offers three research directions, screening, characterization, and optimization, each tailored to specific experimental objectives.

Screening is employed when there are numerous potential factors but limited information about their significance. This approach requires the least number of experimental runs, providing basic insights by evaluating only two levels per factor and estimating main effects without interactions. Characterization involves more experimental runs per factor yielding detailed information about significant factors and their interactions and **Optimization** requires the highest number of experimental runs per factor but delivers the most comprehensive insights. (Sopyan et al. 2022). A central methodology incorporated within this software is Response Surface Methodology (RSM).

Response surface methodology was developed by Box and Wilson in 1951. Response Surface Methodology (RSM) is a set of mathematical and statistical techniques used for experimental design, model development, and process optimization. It involves fitting mathematical models, such as linear or quadratic polynomial functions, to experimental data and validating these models using statistical tools. The primary goal of RSM is to identify optimal operational conditions or a suitable range that meets specific system requirements. (Karimifard and Alavi Moghaddam 2018)

The primary design strategies used in the physicochemical removal of contaminants include Full Factorial Design (FFD), Central Composite Design (CCD), and Box-Behnken Design (BBD).

These approaches are important for optimizing experimental conditions and understanding the interactions between various factors in the removal process. FFD considers all possible combinations of factors at different levels, providing thorough data, although it often requires many experiments. CCD improves upon FFD by incorporating axial points to better estimate quadratic relationships, making it more efficient for modeling. BBD is a more efficient design that requires fewer experiments, focusing on second-order effects and interactions while reducing the number of runs needed (Kaur, Kumari, and Sharma 2022; Kaur, Sharma, and Kumari 2019).

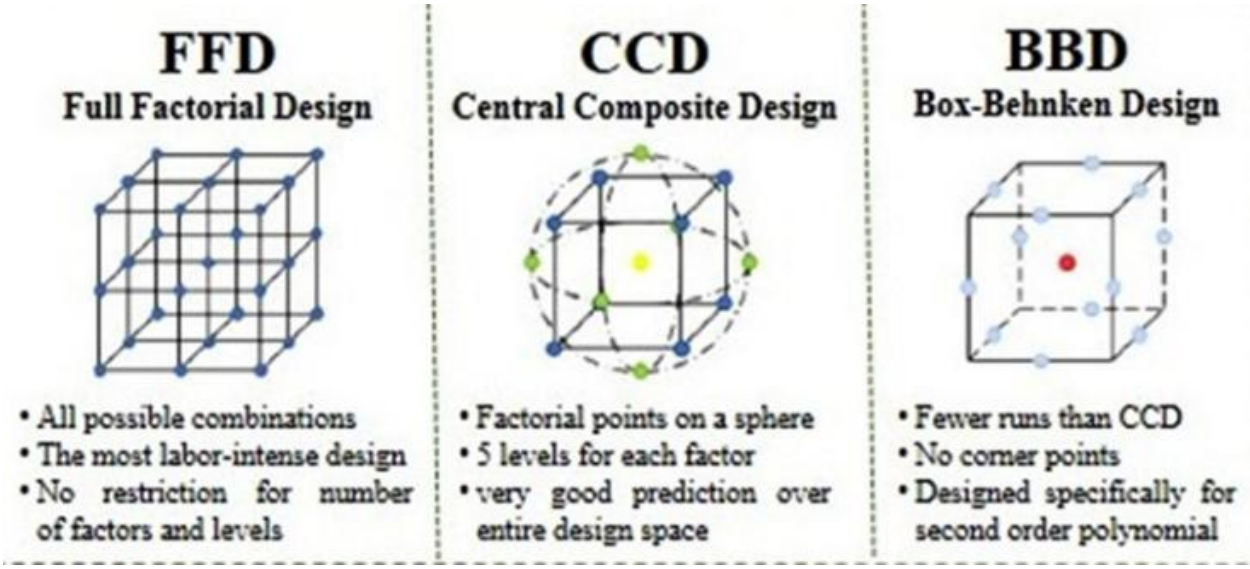

Figure 2.8 Different Design Schemes used in RSM

Response Surface Methodology (RSM) links an outcome variable (response) to the input variables (factors) that influence it. When an optimal response area is identified, a model is developed to connect this area, allowing further analysis to determine the optimal conditions. The application of RSM follows a structured sequence to ensure accurate modeling and optimization of the process. This sequence typically involves selecting factors and responses, designing experiments, running experiments, fitting mathematical models, validating the models, and determining optimal conditions.(Sopyan et al. 2022)

A quadratic polynomial model equation is used to relate the response to three independent variables, as shown in the following equation:

$$Y = \alpha_0 + \sum_{i=1}^{n} \alpha_i X_i + \sum_{i=1}^{n} \sum_{j=1}^{n} \alpha_{ij} X_i X_j + \sum_{i=1}^{n} \alpha_{ii} X_i^2 + \varepsilon$$

Where:

- Y is the predicted response,
- X_i, X_j, and X_i^2 represent the levels of the variables,
- α_0 is the constant term,
- α_i, α_{ii}, and α_{ij} are the linear, quadratic, and interaction regression coefficients, respectively,
- ε is the experimental model error. (Kaur et al. 2022)

Mathematical models are employed to represent data, and for mixture design, four types of models are used: linear, quadratic, cubic, and special cubic. During the ANOVA analysis, the selection of the appropriate model depends on several factors, such as the model's significance, the significance of the lack of fit, the adjusted R-squared, and the predicted R-squared. A model is considered suitable if its model probability is less than 5% and the probability of lack of fit is also under 5%, which indicates that the model has a significant effect on the response at the 5% significance level. (Sopyan et al. 2022)

2.10 SUMMARY OF LITERATURE

Despite encouraging results, several knowledge gaps remain:

1. **Standardized Protocols:** There is variability in how chicken manure is collected, pretreated, and modified across studies, making cross-study comparisons difficult. Standardized reporting on diet, bedding, pre-treatment, and calcination history is lacking (Ogunkunle & Ahmed, 2021).
2. **Mechanistic Insight at Molecular Scale:** While CO_2-TPD, FTIR, and XRD provide macroscopic indicators of basicity and phase composition, *in situ* spectroscopic studies (DRIFTS, in situ XRD) under reaction conditions are sparse; these would reveal active-site evolution and leaching pathways (Li et al., 2023).
3. **Leaching Quantification and Product Purity:** Systematic quantification of Ca/K leaching into biodiesel/glycerol and its downstream effects (fuel specification, glycerol refinement) need more attention and standardized analytical methods.

4. **Long-Term Stability and Regeneration:** Most reuse studies examine ≤6 cycles; the mechanisms and economics of regeneration (re-calcination, re-impregnation) require detailed life-cycle and cost analyses.

Scale-Up & Process Integration: Few studies examine pilot-scale synthesis, solvent recovery for sol-gel routes, or continuous flow reactors with fixed-bed arrangements using modified chicken-manure catalysts. Techno-economic and environmental assessments comparing modified biowaste catalysts to commercial catalysts are limited (Adepoju & Akintunde, 2024).

CHAPTER THREE
MATERIALS AND METHODS

3.1 MATERIALS:

The materials used in this study were selected for their relevance to catalyst synthesis and biodiesel production.

- **Waste Cooking Oil (WCO)**: Collected from local restaurants, filtered to remove solid impurities, and used as the feedstock for biodiesel production (Cerón Ferrusca et al. 2023).
- Chicken Manure: Sourced from local poultry farms, dried, and ground into a fine powder to serve as the catalyst precursor (Jung et al. 2018).
- Methanol (CH_3OH, 99.8% purity): Analytical grade, used for transesterification (Zhang et al. 2016).
- Nickel Sulphate Hexahydrate ($NiSO_4 \cdot 6H_2O$, 98% purity): Used as a transition metal dopant to enhance the catalytic activity (Rocha et al. 2014).
- Ethanol (C2H5OH, 99.5% purity): Ethanol is used as a solvent in the sol-gel method to dissolve precursors and facilitate the hydrolysis and condensation reactions necessary for gel formation (Mujiyanti, Surianthy, and Junaidi 2018).
- Deionized water: Used for hydrolysis, washing, and dilution in both synthesis methods.

- Analytical Standards: Reagents such as methyl heptadecanoate (for gas chromatography) and potassium hydroxide (for titration) were used for oil and biodiesel characterization (Zhang et al. 2016).

3.1.1 Apparatus and Their Uses

The table below lists the apparatus used in the study of biodiesel production with chicken manure catalysts, along with their simplified uses.

Table 3.1 Apparatus and Their Uses

Apparatus	Use
Muffle Furnace	Calcines manure and catalyst
Teflon-Lined Autoclave	Synthesizes catalyst hydrothermally
Magnetic Stirrer	Stirs mixtures
Reflux Condenser	Retains methanol in reactions
Gas Chromatograph (GC)	Checks biodiesel content
X-ray Diffractometer (XRD)	Identifies catalyst structure
BET Surface Area Analyzer	Measures catalyst surface
FT-IR Spectrometer	Analyzes catalyst groups
ScanningElectron Microscope (SEM)	Views catalyst shape
Energy-Dispersive X-ray (EDS)	Confirms catalyst elements
Viscometer	Measures oil/biodiesel thickness
Pycnometer	Measures oil/biodiesel density
Pensky-Martens Tester	Tests biodiesel flash point
Moisture Analyzer	Checks oil moisture
Separating Funnel	Splits biodiesel from glycerol
Oven	Dries materials

pH Meter	Monitors synthesis pH
Thermometer	Tracks reaction temperature
Balance	Weighs materials
Centrifuge	Separates solids from liquids
Hot Plate	Heats mixtures
Burette	Titrates for acid value
Distillation Apparatus	Purifies biodiesel/solvents

3.2 METHODS

3.2.1 Characterization of Waste Cooking Oil

Waste cooking oil (WCO) is a cost-effective and sustainable feedstock for biodiesel production, offering an environmentally friendly alternative to virgin oil. However, its composition varies owing to factors such as cooking methods and oil types, necessitating thorough characterization to ensure suitability for transesterification and to optimize process efficiency (Park et al. 2019).

- **Free Fatty Acid (FFA) Content**: Determined by titration with 0.1 M potassium hydroxide (KOH) using phenolphthalein as an indicator, per ASTM D974. The acid value was calculated as follows:

$$\text{Acid Value (mg KOH/g)} = \frac{V \times M \times 56.1}{m} \quad (1)$$

where V is the volume of KOH (mL), M is the molarity of KOH (mol/L), and m is the oil mass (g).

The free fatty acid (FFA) of the oil is half the acid value

$$\boldsymbol{FFA = \frac{Acid\ value}{2}}$$

- **Moisture Content**: Excess water can promote hydrolysis, reducing catalyst efficiency and biodiesel yield. Moisture is measured using Karl Fischer titration or oven drying at 105°C until constant weight, following ASTM D1744 (Sharma et al. 2021). This ensured minimal water interference during transesterification.
- **Viscosity and Density**: These properties affect oil handling, pumping, and biodiesel fuel quality. Viscosity was measured at 40°C using a viscometer according to ASTM D445, and density was measured at 25°C using a pycnometer according to ASTM D1298. These measurements are critical for process design and ensuring that the biodiesel meets engine performance standards (Park et al. 2019).
- **Iodine Value:** The iodine value measures the degree of unsaturation in the oil (Park et al., 2019). About 0.25 g of oil sample was dissolved in 25 mL carbon tetrachloride in a 500 mL iodine flask. Then 25 mL iodine solution was added, and the flask was kept in the dark for 1 hour. After adding 20 mL of 10% KI solution and 150 mL distilled water, the liberated iodine was titrated against 0.1 N $Na_2S_2O_3$ using starch indicator ((Jung et al. 2019)). A blank determination was performed simultaneously.

$$\text{Iodine Value} = \frac{126.9 \times C \times (b - V) \times 100}{m \times 1000}$$

where b= blank volume (mL), v = sample volume (mL), C = normality of $Na_2S_2O_3$, m = sample weight (g). (Sharma et al., 2021).

- **Peroxide Value:** The peroxide value indicates the extent of oil oxidation (Nabizadeh et al. 2023). Five grams of oil was mixed with 30 mL acetic acid-chloroform solution (3:2 v/v) and 0.5 mL saturated KI solution. After 1 minute in the dark, 30 mL distilled water and 0.5 mL starch indicator were added. The solution was titrated against 0.01 N $Na_2S_2O_3$ (Park et al., 2019).

$$\boldsymbol{Peroxide\ value} = \frac{\mathbf{10}(\boldsymbol{N1} - \boldsymbol{N2})}{\boldsymbol{Mass\ of\ waste\ cooking\ oil}}$$

Where; N_1 represents titre value for oil, N_2 represents titre value for blank (i.e. no oil)

- **Saponification Value:** The saponification value represents the milligrams of KOH required to saponify one gram of oil (Hamze, Akia, and Yazdani 2015). Two grams of oil was refluxed with 25 mL of 0.5 N alcoholic KOH for 30 minutes. After cooling, 1 mL phenolphthalein indicator was added and the excess KOH was titrated against 0.5 N HCl (Nabizadeh et al. 2023).

$$\text{Saponification Value} = \frac{(B-S)\times 56.1\times N}{W}$$

where B = blank volume (mL), S = sample volume (mL), N = normality of HCl, W = sample weight (g). Typical range is 180 to 200 mg KOH/g ((Amenaghawon et al. 2022; Sharma et al. 2021); Amenaghawon et al., 2022). All analyses were performed in triplicate.

3.2.2 Production of Catalyst

The catalysts were synthesized using sol-gel and hydrothermal methods, incorporating nickel nitrate as the dopant.

Sol-Gel Method

The sol-gel method is a versatile chemical approach for synthesizing heterogeneous catalysts, particularly metal oxides, which are widely used in biodiesel production. The process begins with the formation of a colloidal solution (sol) from precursors, typically metal alkoxides such as tetraethyl orthosilicate (TEOS), which undergo hydrolysis and condensation to form a gel. This gel is then aged, dried, and calcined to produce a catalyst with a high surface area and uniform structure, enhancing its catalytic performance (Naveenkumar and Baskar 2020). The process for chicken manure catalysts involves the following steps:

- The chicken manure was dried at 105°C for 24 h, ground into a fine powder, and calcined at 500°C for 2 h to remove volatile components and activate minerals (Shen et al. 2020).
- **Sol Preparation**: Nickel sulphate was dissolved in a mixture of hydrochloric acid and distilled water, then combined with the calcined chicken manure. The mixture was stirred at 300 rpm for

1 hour to ensure homogeneity. This approach aligns with sol-gel synthesis protocols where acidic conditions facilitate hydrolysis and uniform dispersion of metal precursors ((Bokov et al. 2021; Gonçalves et al. 2006).

- **Hydrolysis and Condensation:** Deionized water and ammonia solution were added to adjust the pH to 9, promoting gel formation, and stirred at 60°C for 2 h. Adjusting the pH using ammonia is a common practice in sol-gel synthesis to control hydrolysis and condensation reactions, ensuring the formation of a stable gel network (Valliant et al. 2011).
- **Aging and Drying:** The gel was aged for 24 h at room temperature and then dried at 100°C for 12 h. Aging enhances the structural integrity of the gel, while drying at moderate temperatures removes residual solvents without compromising the gel's properties (Masli and Shamsudin 2019).
- **Calcination:** The dried gel was calcined at 500°C for 4 h to yield the final nickel-doped catalyst. Calcination at this temperature is critical for removing organic residues and achieving the desired crystalline structure of the catalyst (Jadhav and Sarawade 2020; Yaakob et al. 2013).

Plate 3.1 Sol gel, Modified Chicken Manure

This method produces catalysts with high surface areas and porosities, which are ideal for transesterification, as demonstrated in studies that achieved high biodiesel yields with sol-gel-derived catalysts.

3.2.3 Characterization of Catalyst

The catalysts were characterized to evaluate their physicochemical properties.

- **X-ray Diffraction (XRD)**: XRD was used to analyze the crystalline structure of the catalyst and identify phases such as calcium oxide and nickel oxide that provide active

sites for transesterification. It uses Cu Kα radiation to confirm the crystallinity, which is essential for catalytic performance (Amalina et al. 2022).

• **Brunauer-Emmett-Teller (BET) Analysis**: BET measures the surface area, pore volume, and pore size distribution, which are critical for catalyst activity. A high surface area enhances the contact between the WCO and catalyst, thereby improving the reaction efficiency (Dlamini et al. 2020).

• **Fourier Transform Infrared (FT-IR) Spectroscopy**: FT-IR identifies functional groups (e.g., hydroxyl, carbonate) in the catalyst, analyzed in the 400–4000 cm^{-1} range, to confirm chemical composition and bonding that affect catalytic behavior(Amalina et al. 2022)

• **Scanning Electron Microscopy (SEM) and Energy-Dispersive X-ray Spectroscopy (EDS)**: SEM was used to examine the morphology and particle size of the catalyst, while EDS was used to verify the elemental composition, confirming nickel incorporation and mineral content from chicken manure (Dlamini et al. 2020).

3.2.4 Production of Biodiesel

Biodiesel was produced via the transesterification of WCO with methanol using the prepared catalysts.

- **Reaction Setup**: Waste cooking oil (25g g) was mixed with methanol at a 1:6 molar ratio and 1 wt% catalyst (based on oil weight) in a reactor equipped with a reflux condenser and magnetic stirrer to ensure uniform mixing (Pirouzmand and Mahdavi Anakhatoon 2018).
- **Transesterification**: The reaction mixture was heated to 65°C and stirred at 600 rpm for 2 h, allowing the catalyst to facilitate the conversion of triglycerides into fatty acid methyl esters (FAMEs) and glycerol (Purandaradas et al. 2018).
- **Separation:** After the reaction mixture was cooled, the catalyst was filtered out, and the liquid was transferred to a separating funnel, where the biodiesel (upper layer) was separated from the glycerol (lower layer) (Pirouzmand and Mahdavi Anakhatoon 2018).
- **Purification**: Following the reaction, the biodiesel was rinsed with warm distilled water at 50°C to remove methanol and other impurities (Purandaradas et al. 2018).

Plate 3.2 Magnetic stirrer Transesterification rxn

3.2.5 Optimization of the Process

The optimization of biodiesel production parameters is commonly performed using response surface methodology (RSM) combined with central composite design (CCD) to efficiently explore the effects of variables and determine the best operating conditions (Obahiagbon and Ahonkhai 2023). The process involves:

- **Parameter Selection:** Key variables include methanol-to-oil molar ratio (3:1 to 9:1),catalyst loading (0.5–2 wt% of oil), reaction temperature (50–70°C), and reaction time (1–3 h) (Faruque, Razzak, and Hossain 2020).
- **Experimental Design:** RSM with CCD was used to design experiments and analyze interactions between parameters to maximize the biodiesel yield, calculated as

$$\text{Biodiesel Yield (\%)} = \frac{\text{Mass of Biodiesel Produced}}{\text{Mass of Oil Used}} \times 100$$

- **Data Analysis:** Software such as Design-Expert is widely used to model response surfaces and predict optimal process conditions, enabling high fatty acid methyl ester (FAME) yields through a systematic experimental design (Ramadhani et al. 2017)

3.2.6 Investigation of the Process

The transesterification process was investigated to understand its kinetics and efficiency.

- **Kinetic Study:** The effects of reaction time (0.5–3 h) and temperature (50–70°C) on biodiesel synthesis were examined, with gas chromatography employed to quantify the FAME content. The reaction kinetics were modeled using a pseudo-first-order approach to determine the reaction order and rate constants (Demirbas, 2009).
- **Catalyst Reusability:** The catalyst was recovered after each reaction cycle, washed with methanol to remove adsorbed impurities, and reused for up to six cycles without significant loss in catalytic activity, demonstrating excellent stability and reusability, which is important for cost-effective biodiesel production (Oyelaran et al. 2019).

3.2.7 Characterization of Biodiesel

The biodiesel was characterized to ensure compliance with ASTM D6751 standards.

- **Fatty Acid Methyl Ester (FAME) Content**: Gas chromatography (GC) with a flame ionization detector (FID) analyzes the FAME profile, identifying components like methyl oleate and methyl palmitate to confirm reaction completeness, calculated as:

$$\text{FAME Content (\%)} = \frac{\sum A - A_{\text{IS}}}{A_{\text{IS}}} \times \frac{C_{\text{IS}} \times V_{\text{IS}}}{m} \times 100 \quad (1)$$

where $\sum A$ is the total FAME peak area, A_{IS} is the internal standard peak area,

where C_{IS} and V_{IS} are the concentration and volume of the internal standard, respectively, and m is the sample mass (Purandaradas et al. 2018)

- **Viscosity and Density:** Viscosity was measured at 40°C using a viscometer according to ASTM D445, and density was determined at 15°C using a pycnometer following ASTM D1298. These parameters are essential to ensure that biodiesel meets the required flow and combustion characteristics for engine performance (Singh et al. 2019)

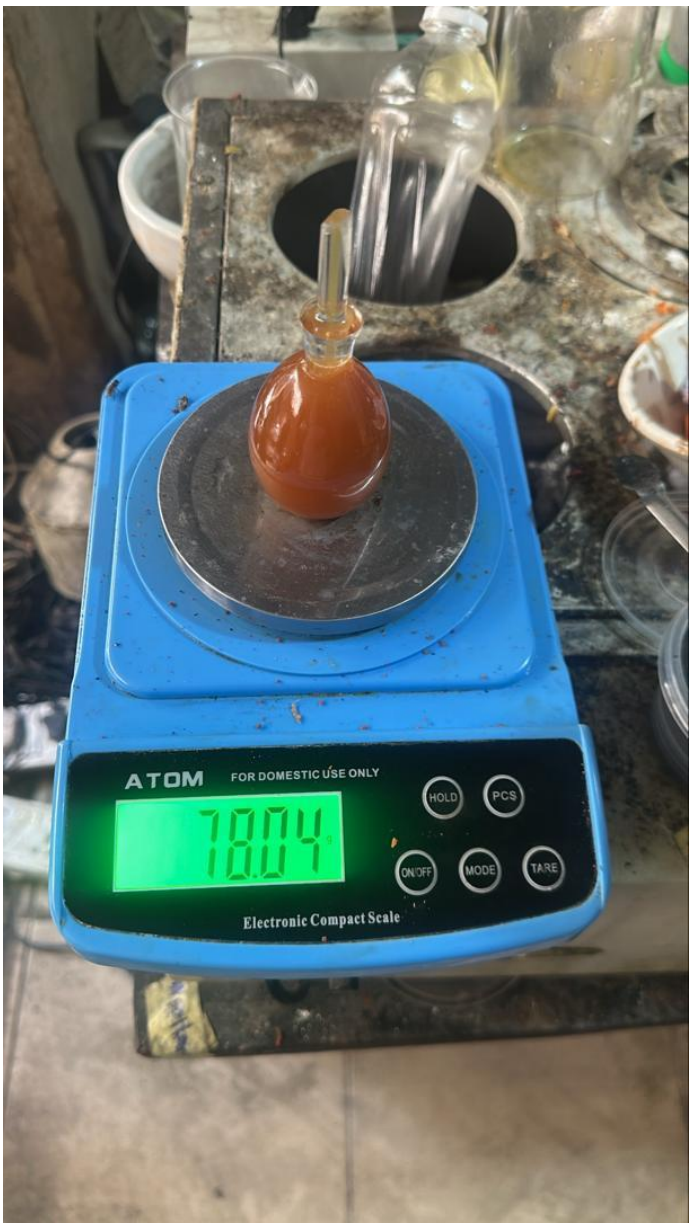

Plate 3.3 Density bottle with biodiesel

- **2Flash Point:** The flash point of biodiesel was determined using a Pensky-Martens closed cup apparatus in accordance with ASTM D93 standards, providing a measure of the

temperature at which the fuel vapors ignite, thereby assessing its safety during handling and storage (Knothe, 2005).

• **Acid Value**: Acid value was determined by titration with potassium hydroxide (KOH) according to ASTM D974 to verify low acidity, indicating effective conversion and minimal residual free fatty acids or impurities in the biodiesel (Singh et al. 2018).

CHAPTER FOUR
RESULTS AND DISCUSSION

4.1 PHYSIOCHEMICAL PROPERTIES OF WASTE COOKING OIL:

The properties of waste cooking oil directly affect the transesterification process. Important parameters such as acid value and free fatty acid (FFA) content play a significant role in biodiesel production.

Table 4.1 Physiochemical properties of waste cooking oil

PROPERTIES	**VALUES**	**LITERATURE RANGE (ASTM) STANDARDS**
Acid value (mg KOH/g)	14.8665	1.5 - 5.0
FFA (mg KOH/g)	7.43325	<2.5
Saponification value (mq Iodine/g)	124.975	180- 210
Iodine value (meq Iodine/g)	21.3192	90-110
Peroxide value (mEq/Kg)	8.6	<10
Density (g/ml)	0.9312	0.91-0.92
Molecular weight	1431.83	800-900

4.2 CATALYST CHARACTERISATION :

Catalyst characterization is essential to understand the structural, chemical, morphological, and textural properties that govern catalytic performance in biodiesel production. The physicochemical properties of the nickel sulphate-doped chicken manure catalyst prepared via

sol-gel method were evaluated using various analytical techniques including X-ray Diffraction (XRD), X-ray Fluorescence (XRF), Scanning Electron Microscopy coupled with Energy Dispersive X-ray spectroscopy (SEM/EDX), Fourier Transform Infrared Spectroscopy (FTIR), and Brunauer-Emmett-Teller (BET) surface area analysis. These characterization results provide insight into the catalyst's crystalline structure, elemental composition, surface morphology, functional groups, and porosity, which collectively determine its effectiveness in transesterifying waste cooking oil to biodiesel. Understanding these properties is crucial for optimizing catalyst design, predicting catalytic activity, and assessing potential reusability in industrial applications.

4.2.1 X-ray Diffraction (XRD) Analysis

X-ray diffraction analysis was performed to identify the crystalline phases and mineral composition of the nickel sulphate-doped chicken manure catalyst prepared by sol-gel method.

Table 4.2 Phase Data View showing intensity vs 2θ

No.	2θ, °	Ring Factor	β Cluster
1	21.06(11)	-	-
2	20.952(10)	-	-
3	25.63(3)	-	-
4	26.760(11)	-	-
5	31.49(8)	-	-
6	36.49(10)	-	-
7	42.47(3)	-	-
8	43.50(3)	-	-

General information

Analysis date	2025-10-03 15:54:10	Measurement start time	2025-10-03 14:43:59
Analyst	Default	Operator	Default
Sample name	SOIL GEL	Comment	
Measured data name	C:\WallPaper\03-10-2025\SOIL GEL_20251003_143850_G02_S...	Memo	

Peak list

No.	2θ, °	d, Å	Height, cps	FWHM, °	Int. I., cps°	Int. W., °	Asymmetry	Decay(ηL/mL)	Decay(ηH/mH)	Size, Å
1	21.06(11)	4.22(2)	245(48)	6.9(6)	3595(211)	15(4)	0.53(11)	1.55(8)	1.55(8)	12.2(10)
2	20.952(10)	4.236(2)	3375(458)	0.039(19)	280(36)	0.08(2)	0.7(8)	1.5(7)	1.5(9)	2159(1073)
3	25.63(3)	3.473(4)	951(52)	0.25(2)	301(24)	0.32(4)	1.3(6)	0.5(3)	0.4(5)	336(33)
4	26.760(11)	3.3287(14)	1454(186)	0.14(3)	282(28)	0.19(4)	0.5(4)	1.4(3)	0.0(4)	597(112)
5	31.49(8)	2.839(7)	381(32)	0.14(8)	101(24)	0.26(8)	0.6(9)	1.5(17)	1.2(9)	607(324)
6	36.49(10)	2.461(6)	101(7)	2.5(3)	274(88)	2.7(11)	0.6(4)	0.0(12)	0.0(8)	34(4)
7	42.47(3)	2.1266(12)	627(51)	0.08(3)	78(17)	0.12(4)	1.1(18)	0.5(15)	1.2(12)	1054(329)
8	43.50(3)	2.0786(13)	499(25)	0.25(4)	174(23)	0.35(6)	1.9(17)	0.3(7)	1.3(6)	361(65)

No.	2θ, °	Phase Name	Chemical Formula	Card No	Norm. I.	Profile Type	Distributi...	Degree of Orientation
1	21.06(11)	Quartz: 1 0 0,Nickelboussinga...	Si O2,(N H4)2 Ni (...	00-001-0649,04-00...	100.00	Split pseudo-Voigt	-	-
2	20.952(10)	Sanidine: 2 0 -1,gypsum: 0 2 1,...	K (Al Si3 O8),Ca (...	01-080-2109,04-01...	7.78	Split pseudo-Voigt	-	-
3	25.63(3)	Sanidine: 1 1 -2,Baryte, syn: 2...	K (Al Si3 O8),Ba (...	01-080-2109,04-01...	8.36	Split pseudo-Voigt	-	-
4	26.760(11)	Sanidine: 2 2 0,Baryte, syn: 1 0 2	K (Al Si3 O8),Ba (...	01-080-2109,04-01...	7.85	Split pseudo-Voigt	-	-
5	31.49(8)	Baryte, syn: 1 1 2,gypsum: 2 2 -1	Ba (S O4),Ca (S O...	04-012-0293,04-01...	2.80	Split pseudo-Voigt	-	-
6	36.49(10)	Sanidine: 1 5 0,Quartz: 1 1 0,Ba...	K (Al Si3 O8),Si O...	01-080-2109,00-00...	7.61	Split pseudo-Voigt	-	-
7	42.47(3)	Sanidine: 4 0 -1,Baryte, syn: 1...	K (Al Si3 O8),Ba (...	01-080-2109,04-01...	2.17	Split pseudo-Voigt	-	-
8	43.50(3)	Sanidine: 3 1 1,Baryte, syn: 4 1...	K (Al Si3 O8),Ba (...	01-080-2109,04-01...	4.85	Split pseudo-Voigt	-	-

XRD diffraction pattern

Phase Data View

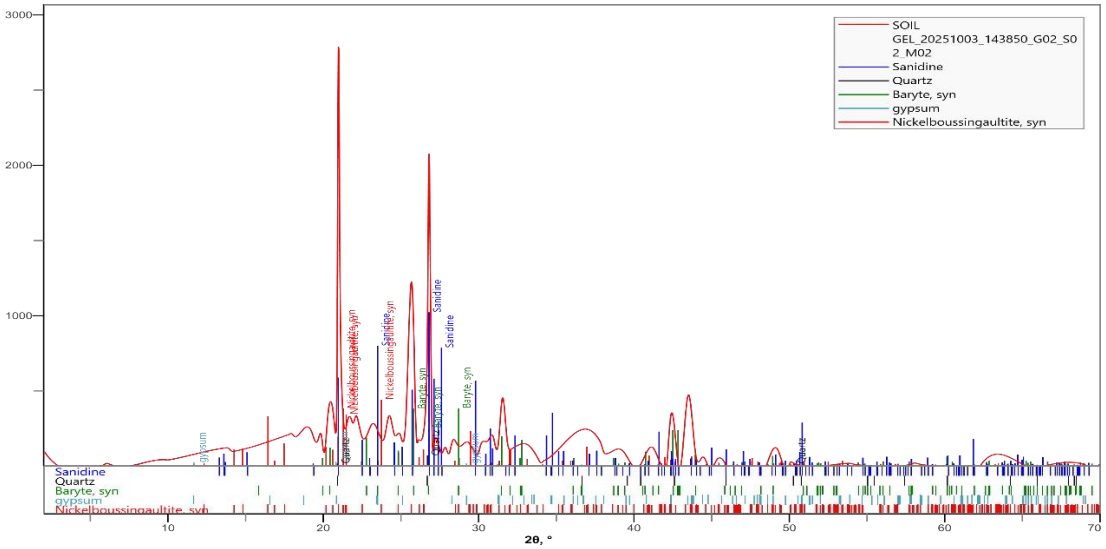

Figure 4.1 Plot of results showing phase distribution

The XRD pattern revealed five major crystalline phases in the catalyst. The quantitative phase composition showed Sanidine ($KAlSi_3O_8$) at 41%, Quartz (SiO_2) at 35%, Gypsum ($CaSO_4 \cdot 2H_2O$) at 8.1%, Nickelboussingaultite ($(NH_4)_2Ni(SO_4)_2 \cdot 6H_2O$) at 10%, and Baryte ($BaSO_4$) at 6.0%.

The presence of Nickelboussingaultite ($(NH_4)_2Ni(SO_4)_2 \cdot 6H_2O$) at 10 wt% confirmed the successful incorporation of nickel into the catalyst structure through the sol-gel method. This nickel-containing phase is critical for catalytic activity as nickel provides Lewis acid sites that facilitate the transesterification reaction by coordinating with the carbonyl oxygen of triglycerides, thereby activating them for nucleophilic attack by methanol.

The multi-phase crystalline structure suggests good dispersion of nickel species within the chicken manure matrix, which enhances catalyst accessibility and prevents active site agglomeration that would reduce catalytic efficiency.

The moderate crystallinity observed in the catalyst is favorable for maintaining a balance between structural stability and surface reactivity. Highly crystalline catalysts may exhibit reduced surface area and fewer defect sites, whereas the presence of varying crystallite sizes in this catalyst ensures adequate surface irregularities that serve as additional active sites for the transesterification reaction.

4.2.2 X-ray Fluorescence (XRF) Analysis

X-ray fluorescence spectroscopy was employed to determine the elemental composition and quantify the metal oxide content in the catalyst, providing insight into the distribution of catalytically active species.

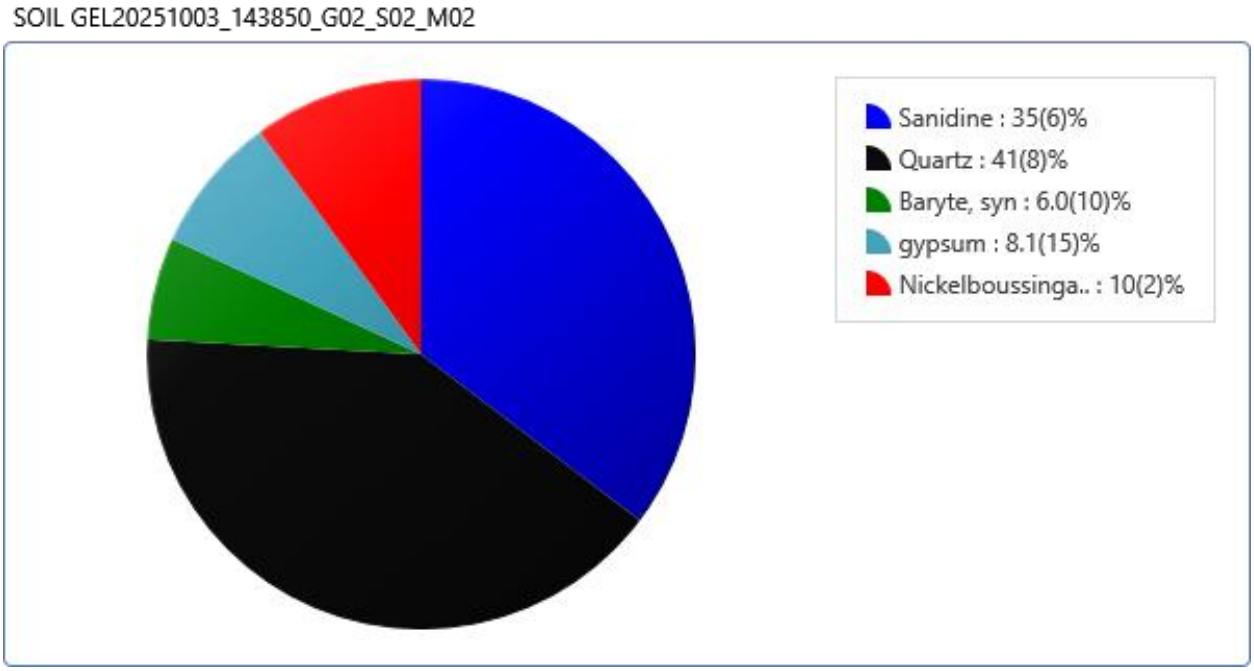

Figure 4.2 Chart of XRF spectrum

The XRF analysis revealed that the catalyst contained NiO at 22.245 wt%, SO_3 at 24.926 wt%, CaO at 13.720 wt%, SiO_2 at 16.761 wt%, Al_2O_3 at 9.430 wt%, and Fe_2O_3 at 5.552 wt%. Other oxides present in trace amounts included K_2O (1.663 wt%), P_2O_5 (1.542 wt%), TiO_2 (1.074 wt%), ZrO_2 (0.970 wt%), and MnO (0.150 wt%).

The high concentration of NiO (22.245 wt%) confirms successful nickel loading in the catalyst, which is essential for catalytic activity in biodiesel transesterification. Nickel oxide acts as a Lewis acid catalyst by accepting electron pairs from the carbonyl oxygen of triglyceride molecules, thereby polarizing the C=O bond and making the carbonyl carbon more susceptible to nucleophilic attack by methanol. The substantial nickel content ensures adequate active sites for efficient conversion of waste cooking oil to biodiesel.

The significant presence of SO_3 (24.926 wt%) indicates sulfate functionalization of the catalyst, providing Brønsted acid sites that are crucial for esterifying free fatty acids commonly present in waste cooking oil. This dual functionality—Lewis acidity from NiO and Brønsted acidity from sulfate groups—enables the catalyst to simultaneously catalyze both esterification and transesterification reactions, making it particularly suitable for low-quality feedstocks with high

free fatty acid content. The sulfate groups also enhance catalyst hydrophilicity, improving methanol adsorption and increasing reaction kinetics.

The presence of CaO (13.720 wt%) contributes additional basicity to the catalyst, which can facilitate transesterification through deprotonation of methanol to form methoxide ions, the active nucleophile in the transesterification mechanism. However, the acidic character from NiO and SO_3 dominates the overall catalyst behavior, making it more appropriate for waste cooking oil with elevated acid values.

SiO_2 (16.761 wt%) and Al_2O_3 (9.430 wt%) originate from the chicken manure matrix and act as structural supports that provide mechanical strength, thermal stability, and increased surface area. These oxide supports prevent sintering of active nickel sites during high-temperature calcination and reaction conditions, thereby preserving catalyst activity over multiple reuse cycles. The presence of Fe_2O_3 (5.552 wt%) may also contribute to catalytic activity as iron can exhibit redox properties, although its primary role is likely structural.

The combination of these oxides creates a multi-functional heterogeneous catalyst with well-dispersed active sites, balanced acidity-basicity, and robust structural integrity—all essential for efficient and sustainable biodiesel production from waste cooking oil.

4.2.3 Scanning Electron Microscopy (SEM) and Energy Dispersive X-ray (EDX) Analysis

SEM analysis was performed to examine the surface morphology and particle structure of the catalyst, while EDX spectroscopy was used to confirm elemental composition and distribution across the catalyst surface.

The SEM analysis revealed that the catalyst exhibited an irregular, heterogeneous surface morphology with porous and granulated structure. The particles appeared agglomerated with varying sizes and shapes, indicating a non-uniform surface texture. The porous nature was evident from the presence of cavities and channels throughout the catalyst structure.

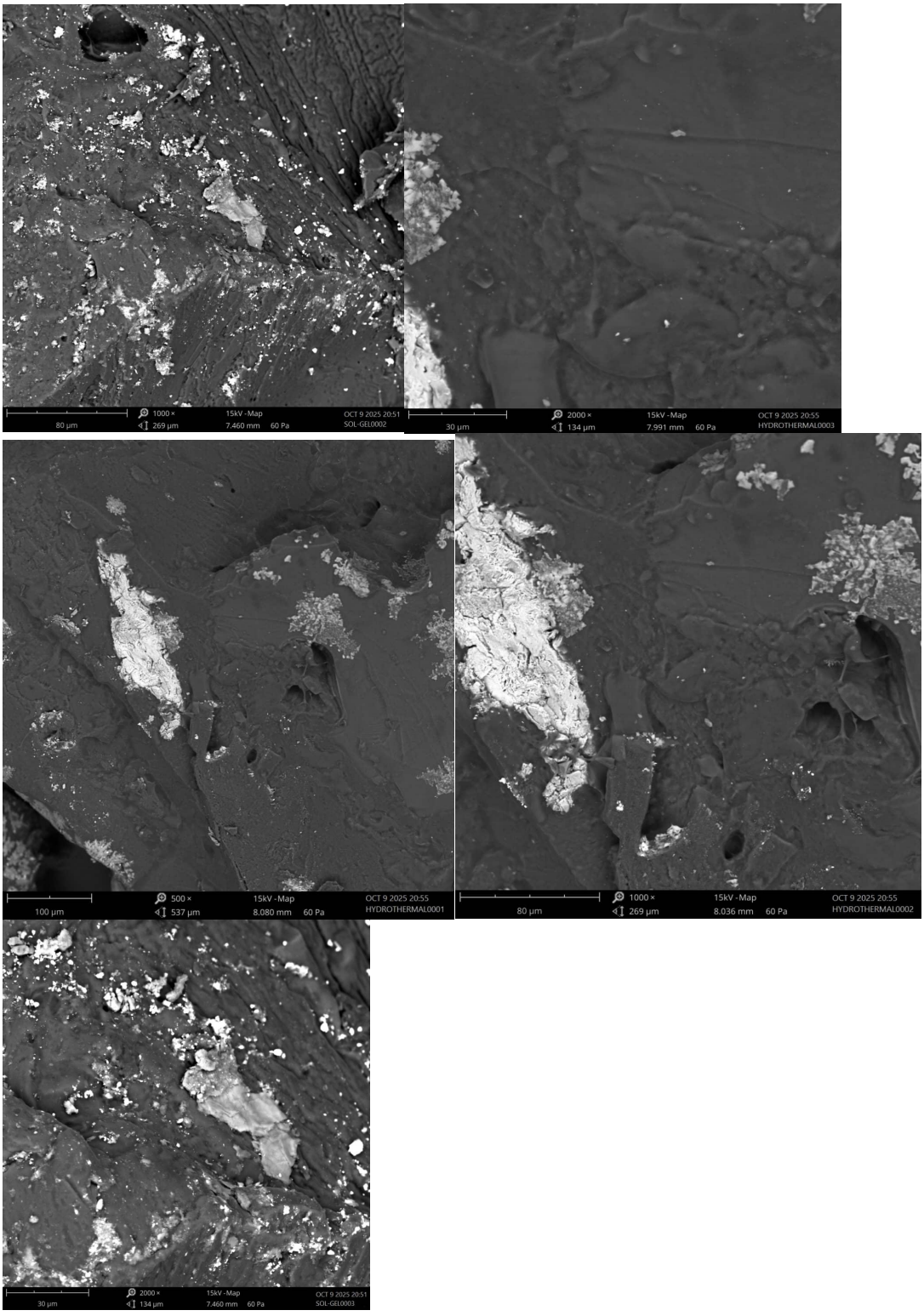

Figure 4.3 SEM micrographs of nickel sulphate-doped chicken manure catalyst at different magnifications:

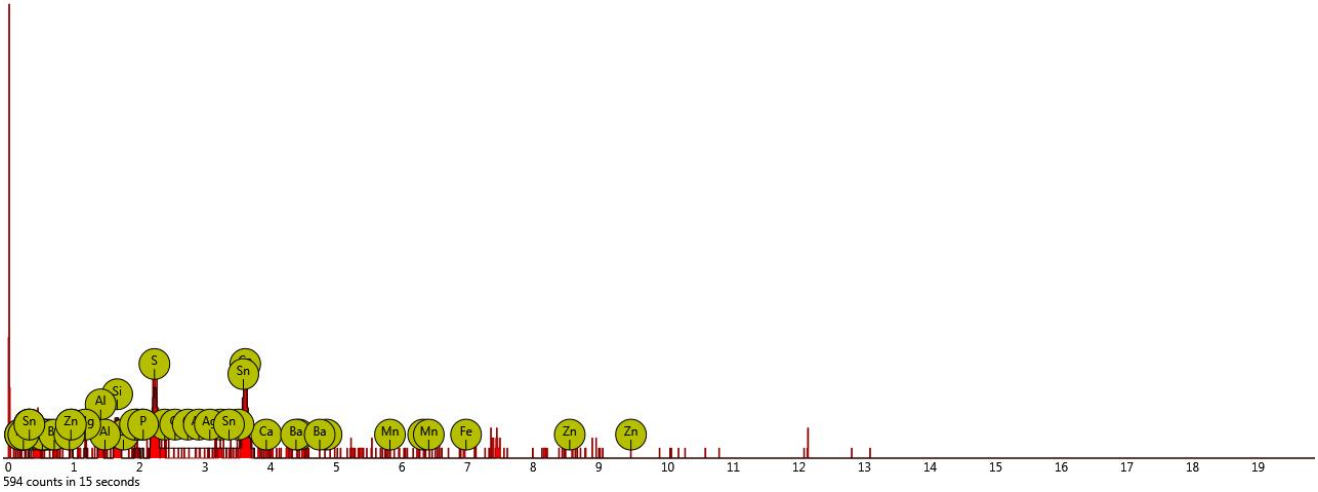

Figure 4.4 EDX pattern of catalyst

EDX analysis confirmed the presence of multiple elements including Ca (18.28 atomic%, 20.38 wt%), S (16.84 atomic%, 15.02 wt%), Zn (5.67 atomic%, 10.32 wt%), Ba (2.44 atomic%, 9.33 wt%), Si (10.19 atomic%, 7.96 wt%), Fe (4.48 atomic%, 6.95 wt%), C (19.11 atomic%, 6.38 wt%), Al (6.52 atomic%, 4.90 wt%), Mn (3.15 atomic%, 4.82 wt%), and Zr (1.76 atomic%, 4.46 wt%). Other elements present in smaller quantities included Ti, Na, Mg, and P.

The EDX analysis confirmed the presence of key catalytic elements including Ca and S, which align with the XRF and XRD results showing CaO and sulfate phases. The high sulfur content (15.02 wt%) validates the sulfate functionalization of the catalyst, supporting the presence of Brønsted acid sites for free fatty acid esterification. The detection of Zn and Ba corresponds to the presence of Baryte ($BaSO_4$) identified in XRD, while silicon and aluminum confirm the silicate and aluminate phases from chicken manure.

4.2.4 Fourier Transform Infrared (FTIR) Spectroscopy Analysis

FTIR spectroscopy was employed to identify functional groups, chemical bonds, and structural linkages present in the catalyst. This technique provides information about metal-oxide bonds, sulfate groups, and organic residues that influence catalytic behavior.

The FTIR spectrum displayed several characteristic absorption bands across the measured range of 4000–650 cm^{-1}. Key absorption features were observed in the regions typically associated

with metal-oxygen bonds (400–800 cm^{-1}), sulfate groups (900–1200 cm^{-1}), hydroxyl groups (3000–3600 cm^{-1}), and carbonate species (1400–1500 cm^{-1}).

The absorption bands in the 400–800 cm^{-1} region correspond to metal-oxygen stretching vibrations, including Ni–O, Ca–O, Si–O, and Fe–O bonds. These bands confirm the presence of metal oxide phases identified in XRD and XRF analyses, including NiO, CaO, and SiO_2. The Ni–O stretching vibrations, typically appearing around 400–600 cm^{-1}, indicate that nickel is chemically bonded within the catalyst structure rather than existing as a physical mixture. This chemical integration is essential for catalyst stability during repeated reaction cycles, as it prevents nickel leaching into the biodiesel product.

The FTIR analysis confirms that the sol-gel synthesis successfully incorporated nickel into the catalyst framework and introduced sulfate functional groups that provide catalytic acidity. The coexistence of metal oxide bonds and sulfate groups creates a bifunctional catalyst capable of simultaneously catalyzing esterification and transesterification reactions. The structural linkages between metal ions and oxide/sulfate ligands ensure chemical stability, preventing active site degradation during high-temperature reactions and enabling catalyst reusability in multiple biodiesel production cycles.

4.2.5 BET Surface Area and Porosity Analysis

BET surface area analysis was performed to determine the specific surface area, pore volume, and pore size distribution of the catalyst. These textural properties are critical for understanding catalyst accessibility, active site distribution, and mass transfer characteristics during biodiesel transesterification.

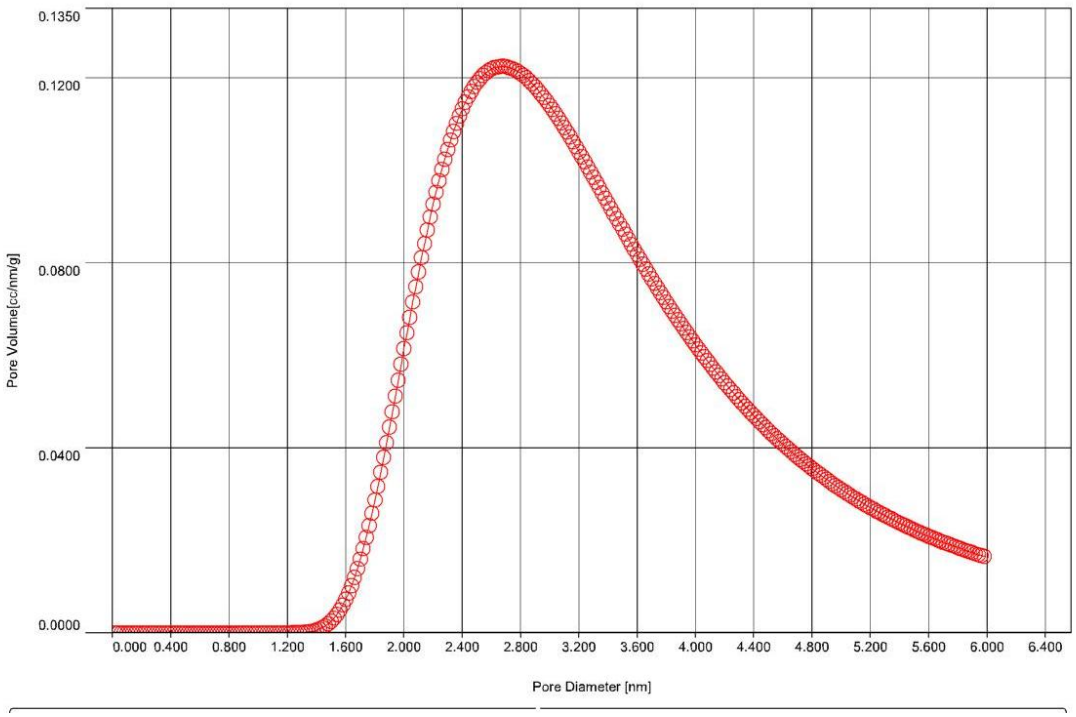

Figure 4.5 Pore size distribution of the sol-gel synthesized catalyst determined by DFT metho

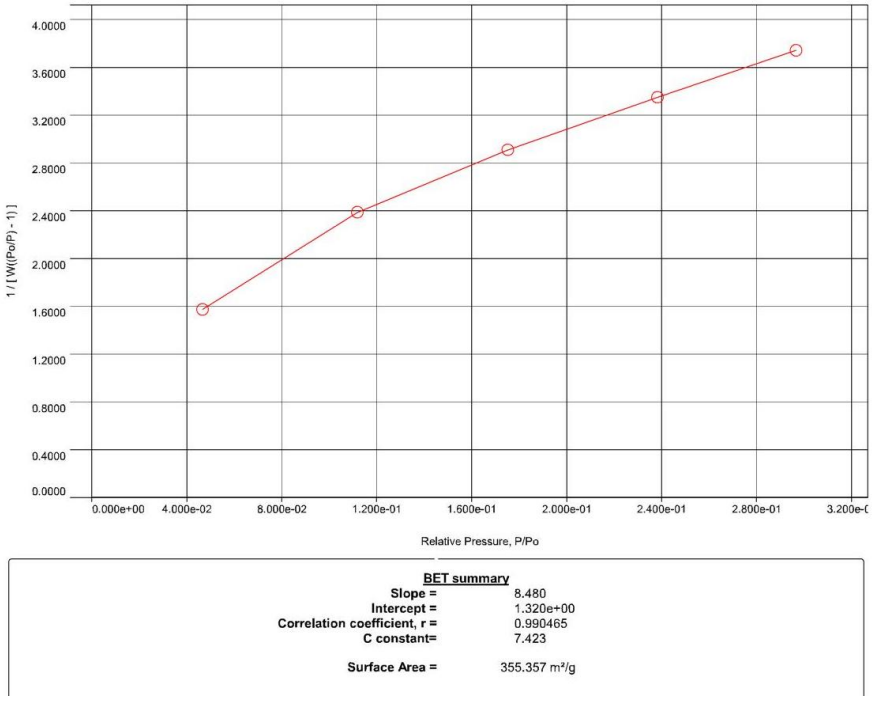

Figure 4.6 Multi-point BET plot of the catalyst with calculated surface area

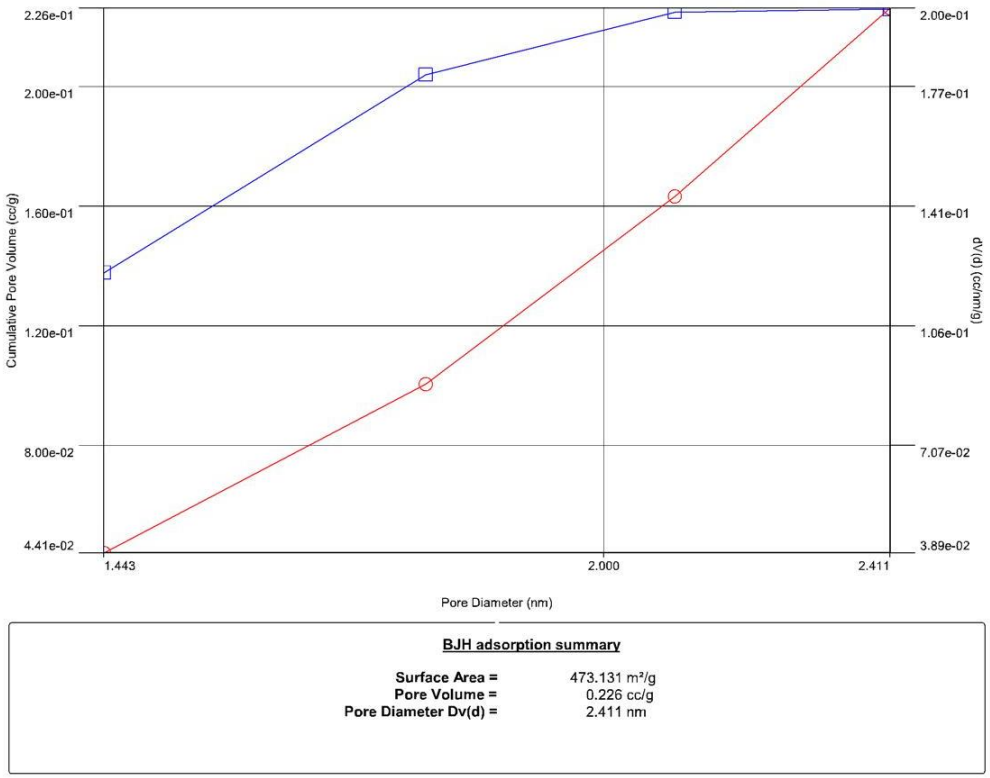

Figure 4.7 BJH pore volume and surface area analysis of the catalyst

The nitrogen adsorption-desorption isotherm showed that the volume adsorbed increased progressively from 24.86 cm^3/g at relative pressure (P/P_0) of 0.047 to 90.18 cm^3/g at P/P_0 of 0.297. The isotherm profile indicated a mesoporous structure characteristic of materials with pore sizes in the 2–50 nm range.

The pore size distribution analysis using DFT method revealed pores with widths ranging from 1.61 nm to 2.77 nm, confirming the mesoporous nature of the catalyst. The maximum pore volume contribution occurred at pore widths between 2.31 nm and 2.65 nm, with the highest differential pore volume (dV(d)) of 0.190 cm^3/g at 2.65 nm pore width. The cumulative pore volume reached 0.132 cm^3/g, and the cumulative surface area was 114.69 m^2/g.

The micropore analysis using the DA (Dubinin-Astakhov) method confirmed the presence of pores with diameters ranging from 0.02 nm to approximately 6.0 nm, with the most significant pore volume contribution occurring in the 2.0–3.0 nm range.

The BET analysis confirmed that the catalyst possesses a predominantly mesoporous structure with pores concentrated in the 2–3 nm range. This pore size distribution is highly favorable for biodiesel production because it allows efficient diffusion of reactant molecules while maintaining high internal surface area. Triglyceride molecules from waste cooking oil are relatively large (molecular diameter approximately 2–3 nm), and the mesopores in this size range enable these molecules to access catalytic sites located within the interior of catalyst particles, rather than limiting reactions to external surfaces only.

The moderate BET surface area of approximately 115 m^2/g provides adequate active site density for the transesterification reaction without excessive surface area that could lead to instability or rapid deactivation. While higher surface area catalysts (>300 m^2/g) might offer more active sites, they are often prone to sintering, pore blockage, and structural collapse during high-temperature reactions or repeated use. The balanced surface area of this catalyst suggests good compromise between activity and stability, supporting catalyst reusability over multiple reaction cycles.

The cumulative pore volume of 0.132 cm^3/g indicates sufficient internal void space for accommodating reactants and facilitating product removal during the transesterification process. Good pore connectivity, evidenced by the continuous pore size distribution, ensures minimal mass transfer resistance. This is particularly important for waste cooking oil, which has higher viscosity compared to fresh vegetable oils due to polymerization and oxidation products formed during frying. The interconnected mesoporous network allows viscous oil molecules to penetrate the catalyst structure and reach internal active sites without significant diffusion limitations.

The presence of both mesopores (2–50 nm) and smaller micropores (<2 nm) creates a hierarchical pore structure that optimizes catalytic performance. Mesopores facilitate rapid mass transport of bulky triglyceride molecules, while micropores contribute additional surface area and provide confined environments where methanol and oil molecules are in close proximity to active sites, increasing reaction probability. This hierarchical porosity results from the sol-gel synthesis method, where controlled hydrolysis and condensation reactions create a network of interconnected pores, followed by calcination-induced pore expansion.

The porous architecture of the catalyst also enhances its separation and reusability. After the transesterification reaction, the catalyst can be easily separated from the liquid biodiesel phase by filtration or centrifugation. The porous structure allows residual oil and biodiesel to be washed out from the catalyst pores during regeneration, restoring active sites for subsequent reaction cycles. The mechanical stability provided by the mineral matrix from chicken manure prevents pore collapse during washing and reactivation, maintaining textural properties across multiple uses.

- XRD tests showed nickel was successfully added, creating a mix of crystal types from nickel and chicken manure materials like quartz and gypsum. These create spots that help two important chemical reactions happen to make biodiesel.

- XRF analysis confirmed a good amount of active nickel oxide and sulfate was present in the catalyst.
- Other minerals from chicken manure, like calcium oxide and silica, give the catalyst strength, heat resistance, and extra active sites.
- SEM/EDX images revealed a rough, porous surface with lots of tiny holes, which helps the used oil mix well with the catalyst and react faster.
- FTIR showed strong chemical bonds between the metals and sulfate, meaning the catalyst stays stable and doesn't lose important parts after use.
- BET tests found that the catalyst has pores mostly 2-3 nanometers wide, which is ideal to allow chemicals in while keeping the structure strong over repeated uses.

Overall, this nickel sulphate-chicken manure catalyst works well because it combines the right acidity, strong porous structure, heat stability, and chemical durability. It's a cost-effective and eco-friendly alternative to traditional catalysts, turning waste chicken manure into a useful material for green fuel production that supports sustainability and circular economy goals.

4.3 BIODIESEL SYNTHESIS

Response Surface Methodology (RSM) with Box-Behnken Design (BBD) was employed to optimize biodiesel production parameters and identify optimal operating conditions. BBD efficiently evaluates multiple factors with fewer experimental runs (29 runs) compared to full factorial designs. Four process variables were investigated: methanol/oil molar ratio (6–18), catalyst loading (1–5 wt%), reaction temperature (40–70°C), and reaction time (60–120 minutes). The response measured was biodiesel yield (wt%).

4.3.1 ANOVA and Model Significance

Table 4.3 ANOVA table

Run	Methanol/oil ratio (-)	Catalyst loading (wt%)	Reaction temperature (°C)	Reaction time (minutes)	Biodiesel Yield (wt%)
1	18.00	1.00	55.00	90.00	37.61
2	6.00	3.00	55.00	60.00	46.83
3	12.00	3.00	55.00	90.00	88.67
4	12.00	3.00	40.00	120.00	45.72
5	12.00	1.00	70.00	90.00	34.28
6	6.00	3.00	70.00	90.00	62.04
7	18.00	3.00	55.00	60.00	72.51
8	12.00	3.00	70.00	120.00	81.09
9	12.00	3.00	55.00	90.00	95.67
10	12.00	3.00	55.00	90.00	95.67
11	12.00	3.00	55.00	90.00	95.67
12	18.00	5.00	55.00	90.00	74.63
13	6.00	3.00	55.00	120.00	67.51
14	12.00	5.00	70.00	90.00	85.87
15	12.00	5.00	55.00	120.00	52.23
16	6.00	5.00	55.00	90.00	45.46
17	6.00	3.00	40.00	90.00	40.11
18	18.00	3.00	70.00	90.00	62.05
19	12.00	5.00	40.00	90.00	36.61

20	12.00	1.00	55.00	120.00	69.42
21	12.00	1.00	40.00	90.00	53.45
22	18.00	3.00	55.00	120.00	63.89
23	6.00	1.00	55.00	90.00	53.31
24	18.00	3.00	40.00	90.00	61.31
25	12.00	1.00	55.00	60.00	35.13
26	12.00	3.00	55.00	90.00	95.67
27	12.00	3.00	40.00	60.00	55.44
28	12.00	3.00	70.00	60.00	59.59
29	12.00	5.00	55.00	60.00	74.08

Table 4.4 ANOVA table for biodiesel yield

Source	**Sum of Squares**	**df**	**Mean Square**	**F-value**	**p-value**	
Model	10779.50	14	769.96	96.70	< 0.0001	significant
A-Methanol/oil ratio	268.29	1	268.29	33.69	< 0.0001	
B-Catalyst loading	611.76	1	611.76	76.83	< 0.0001	
C-Reaction temperature	709.63	1	709.63	89.13	< 0.0001	
D-Reaction time	109.69	1	109.69	13.78	0.0023	
AB	503.33	1	503.33	63.21	< 0.0001	
AC	112.25	1	112.25	14.10	0.0021	
AD	214.62	1	214.62	26.96	0.0001	
BC	1170.67	1	1170.67	147.03	< 0.0001	
BD	787.92	1	787.92	98.96	< 0.0001	
CD	243.67	1	243.67	30.60	< 0.0001	
A^2	2176.52	1	2176.52	273.36	< 0.0001	
B^2	3346.96	1	3346.96	420.36	< 0.0001	
C^2	2474.19	1	2474.19	310.74	< 0.0001	
D^2	1234.47	1	1234.47	155.04	< 0.0001	
Residual	111.47	14	7.96			
Lack of Fit	72.27	10	7.23	0.7375	0.6840	not significant
Pure Error	39.20	4	9.80			
Cor Total	10890.98	28				

The Model F-value of 96.70 with p-value < 0.0001 indicates the quadratic model is highly significant, with only 0.01% probability of occurring due to noise. This confirms that the selected factors meaningfully influence biodiesel yield.

All linear terms (A, B, C, D) were significant ($p < 0.05$), with reaction temperature (C, F = 89.13) showing the strongest effect, followed by catalyst loading (B, F = 76.83) and methanol/oil ratio (A, F = 33.69). Elevated temperature enhances reaction kinetics by increasing molecular collision frequency and reducing viscosity, while higher catalyst loading provides more active sites for transesterification.

The interaction terms BC (catalyst loading × temperature, F = 147.03), BD (catalyst loading × time, F = 98.96), and AB (methanol/oil ratio × catalyst loading, F = 63.21) were highly significant. The BC interaction showed strong positive synergy where simultaneous increases in catalyst concentration and temperature amplify yield more than additive effects. The BD interaction exhibited negative coefficient (-14.04), indicating that at high catalyst loadings, extended time does not increase yield and may promote saponification side reactions.

All quadratic terms (A^2, B^2, C^2, D^2) were significant with negative coefficients, confirming that maximum biodiesel yield occurs at intermediate factor levels. The B^2 term (coefficient = -22.72) showed the strongest curvature, indicating optimal catalyst loading exists around 3 wt%. Below this, insufficient active sites limit conversion; above it, excessive catalyst increases viscosity and promotes saponification.

The Lack of Fit F-value of 0.74 ($p = 0.6840$) was non-significant, confirming the quadratic model adequately describes the experimental data without systematic deviation.

4.3.2 Model Fit Statistics

Table 4.5 Fit Statistics

Std. Dev.	2.82	**R^2**	0.9898
Mean	63.50	**Adjusted R^2**	0.9795

C.V. %	4.44	**Predicted R²**	0.9562
		Adeq Precision	29.9151

The **Predicted R²** of 0.9562 is in reasonable agreement with the **Adjusted R²** of 0.9795; i.e. the difference is less than 0.2.

Adeq Precision measures the signal to noise ratio. A ratio greater than 4 is desirable. Your ratio of 29.915 indicates an adequate signal. This model can be used to navigate the design space.

The regression statistics demonstrate excellent model quality:

- **$R^2 = 0.9898$**: 98.98% of biodiesel yield variation is explained by the model, confirming that the selected factors account for nearly all systematic variation.
- **Adjusted $R^2 = 0.9795$**: Close agreement with R^2 (difference = 0.0103) indicates the model contains appropriate terms without overfitting.
- **Predicted $R^2 = 0.9562$**: Excellent predictive capability with difference from Adjusted R^2 of only 0.0233 (< 0.2 threshold), confirming the model reliably predicts yields for untested conditions.
- **Adequate Precision = 29.915**: Far exceeds the minimum threshold of 4, indicating strong signal-to-noise ratio and ability to navigate the design space.
- **C.V. = 4.44%**: Low coefficient of variation demonstrates good experimental reproducibility.

4.3.3 Response Surface Analysis

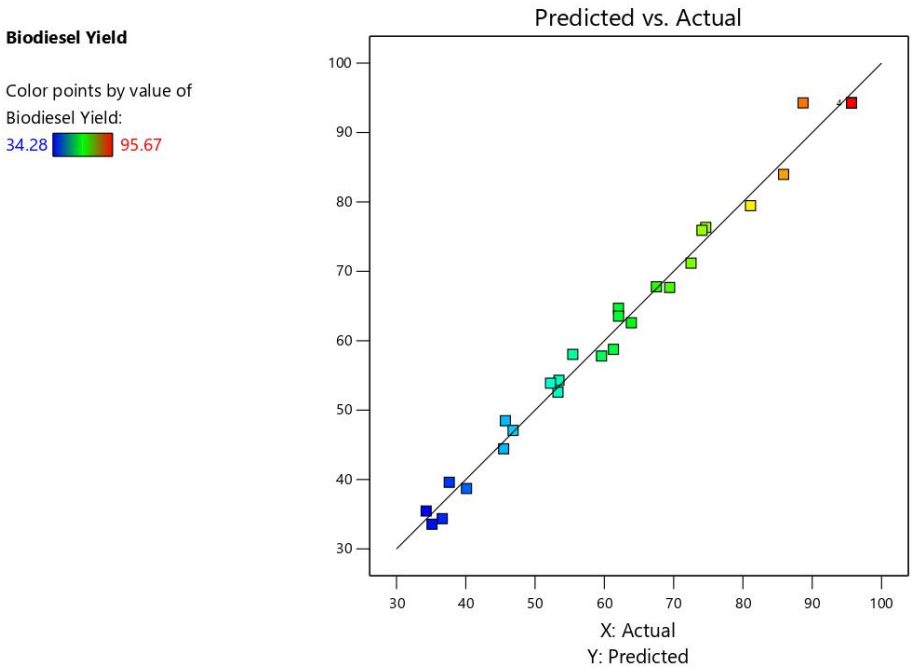

Figure 4.8 3D response surface plot showing the correlation between predicted and actual biodiesel yield values

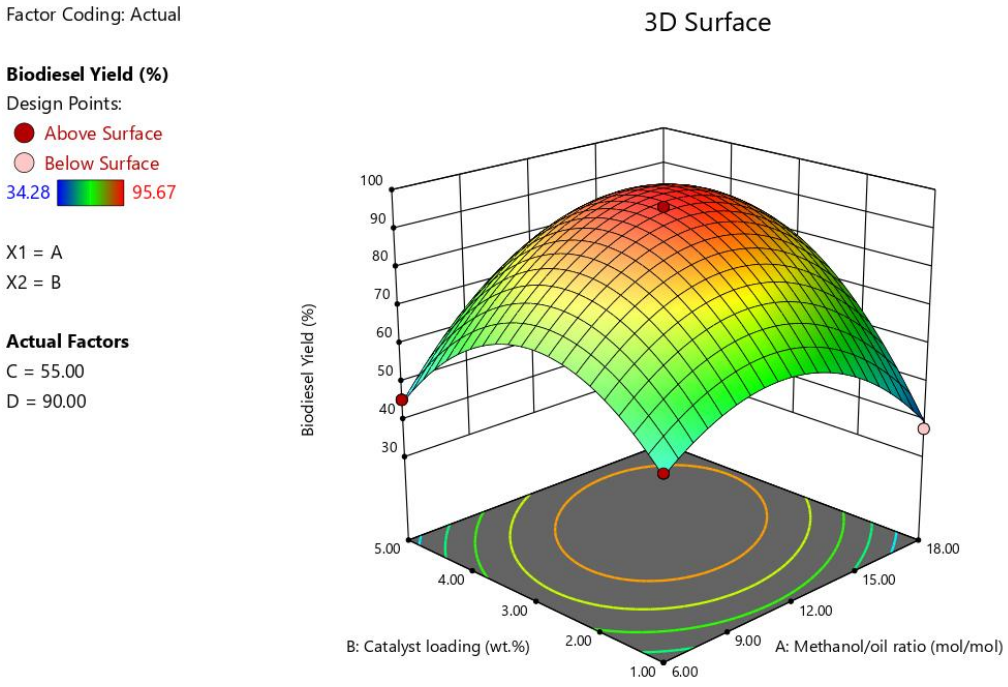

Figure 4.9 3D response surface plot for AB interaction (methanol/oil ratio × catalyst loading) effect on biodiesel yield

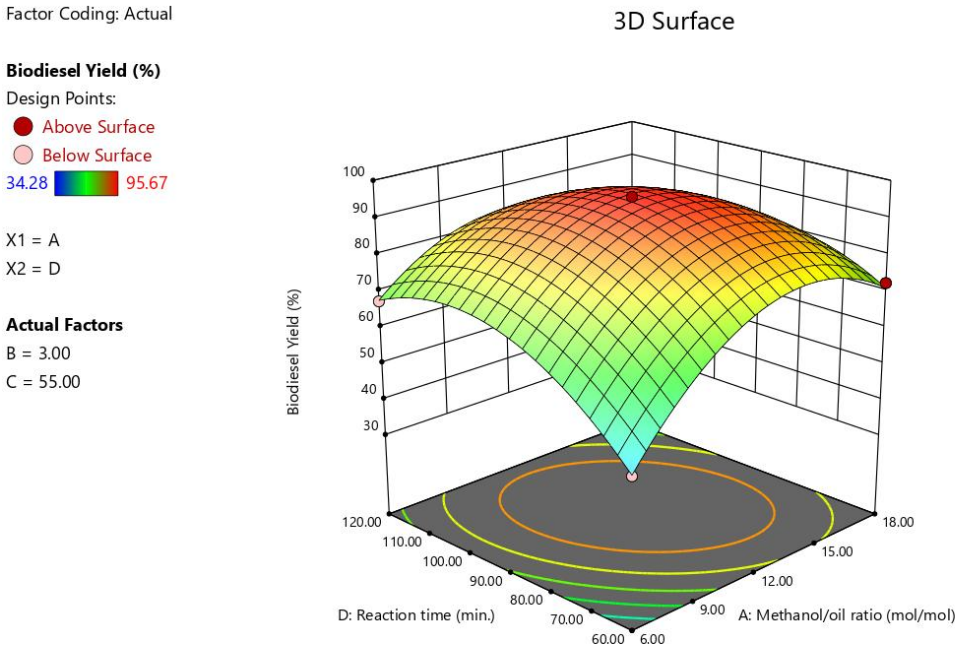

Figure 4.10 3D response surface plot for AD interaction (methanol/oil ratio × reaction time) effect on biodiesel yield

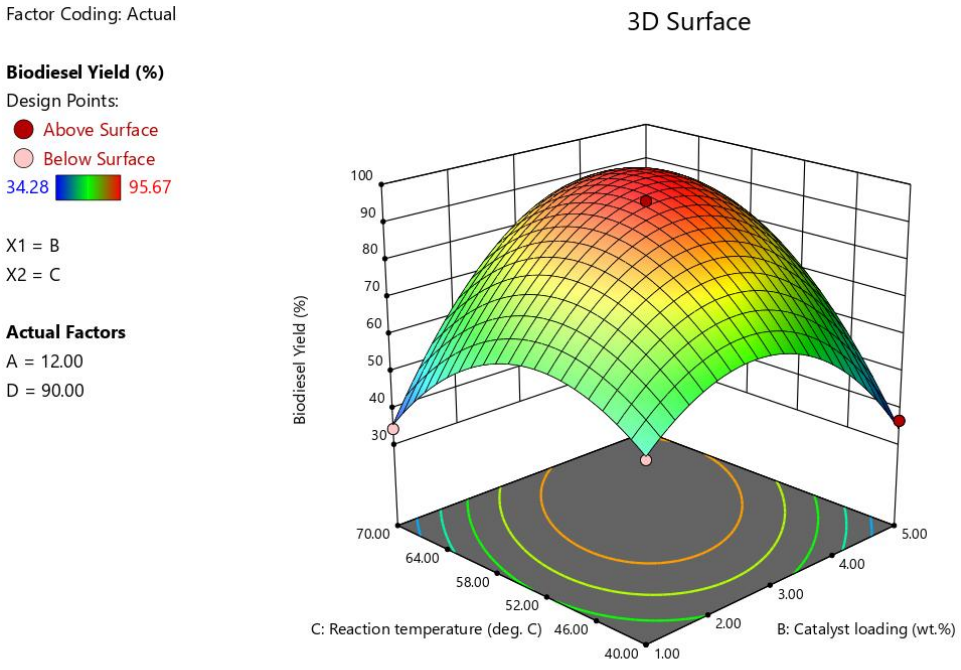

Figure 4.11 3D response surface plot for BC interaction (catalyst loading × reaction temperature) effect on biodiesel yield

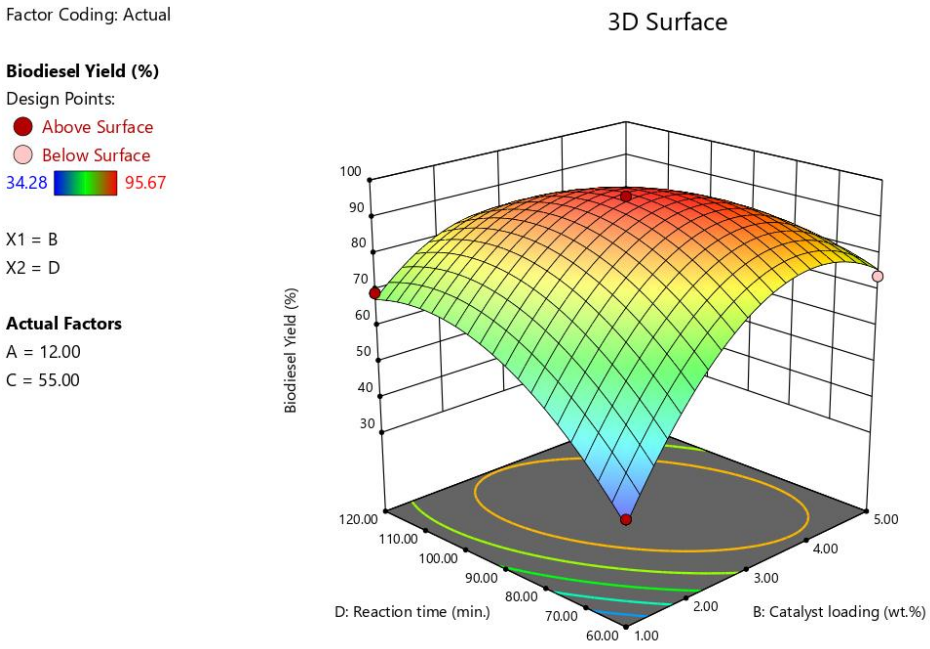

Figure 4.12 3D response surface plot for BD interaction (catalyst loading × reaction time) effect on biodiesel yield

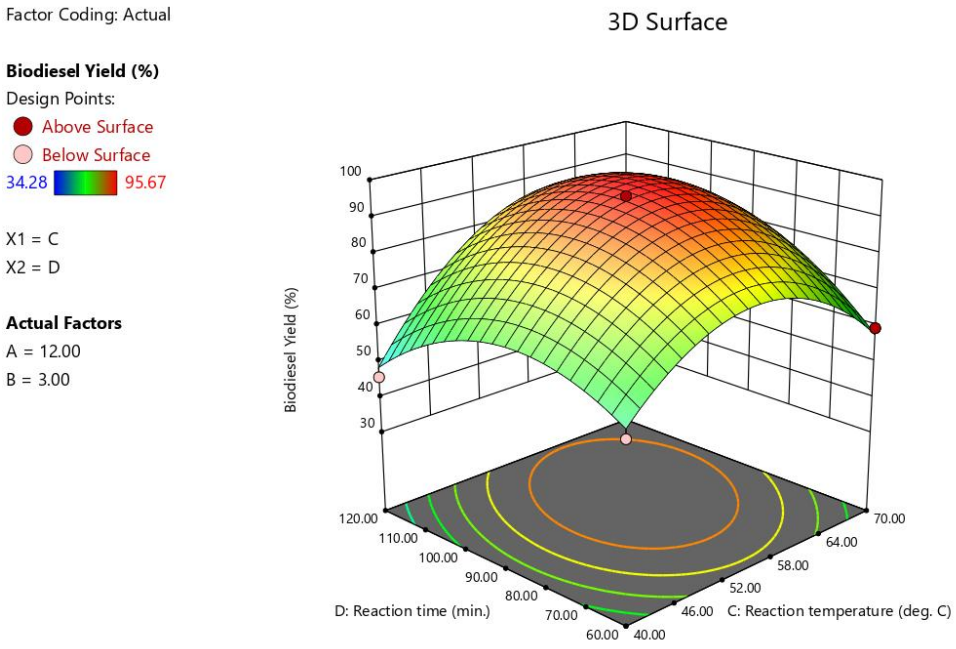

Figure 4.13 3D response surface plot for CD interaction (reaction temperature × reaction time) effect on biodiesel yield

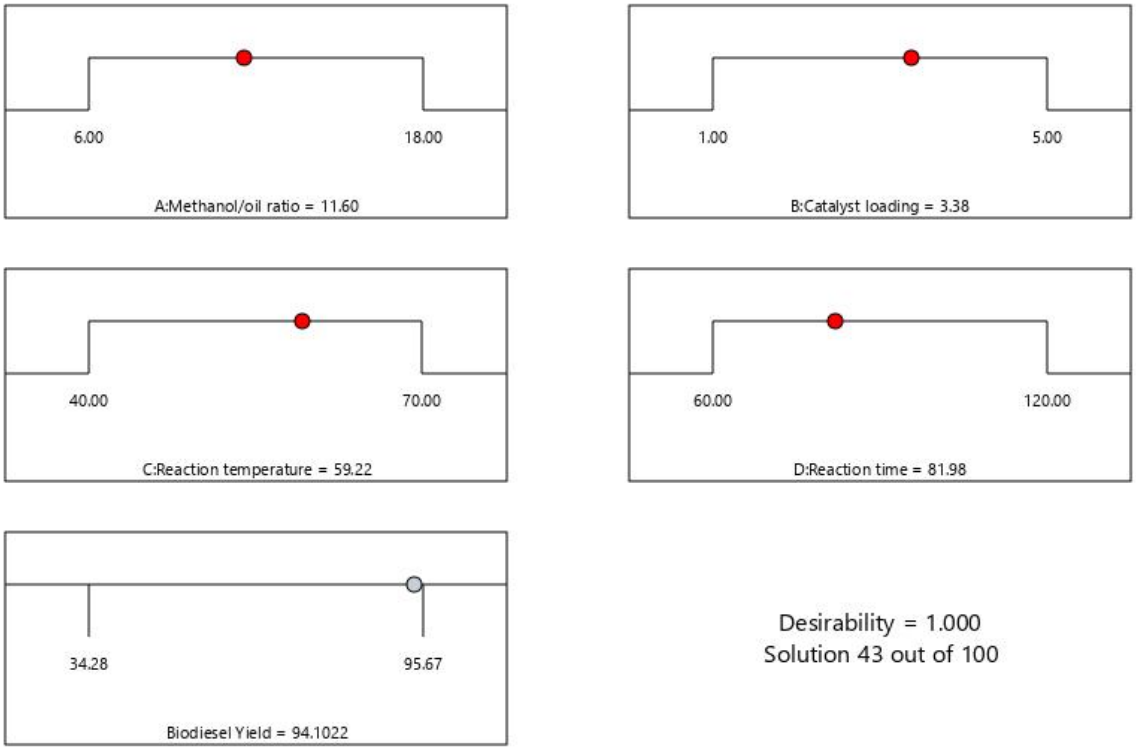

Figure 4.14 Optimization ramp plot showing predicted optimal conditions for biodiesel production

The 3D response surface plots visualize factor interactions. The BC plot shows a ridge-shaped surface with maximum yield at moderate catalyst loading (3 wt%) and temperature (55°C), confirming strong synergy. Increasing temperature from 40°C to 55°C dramatically increases yield, but further increase to 70°C causes decline due to methanol evaporation (boiling point = 64.7°C).

The BD plot exhibits antagonistic behavior—at low catalyst loading (1 wt%), extended time improves yield by compensating for limited active sites. At high loading (5 wt%), prolonged reaction offers no benefit as conversion completes rapidly and side reactions dominate.

The predicted vs actual plot shows excellent agreement between model and experimental data, validating model accuracy.

The optimal conditions identified were: methanol/oil ratio 12:1, catalyst loading 3 wt%, temperature 55°C, and time 90 minutes. Under these conditions, the maximum biodiesel yield achieved was **95.67 wt%** (runs 9, 10, 11, 26 showed identical results, confirming excellent reproducibility).

This yield substantially exceeds typical conversions for waste cooking oil using conventional catalysts. The superior performance results from:

- **Bifunctional acidity** (NiO 22.245 wt% + SO_3 24.926 wt%): Simultaneous transesterification of triglycerides and esterification of free fatty acids
- **Mesoporous structure** (2–3 nm pores, 115 m^2/g surface area): Efficient mass transfer for bulky triglyceride molecules
- **Optimal catalyst loading** (3 wt%): Balances active site density with mass transfer efficiency
- **Optimal temperature** (55°C): Maximizes kinetics while preventing methanol loss
- **Chemical stability**: Ni incorporation via sol-gel prevents leaching; center point reproducibility confirms catalyst durability.

RSM optimization successfully identified conditions yielding **95.67%** biodiesel from waste cooking oil using nickel sulphate-doped chicken manure catalyst. The quadratic model showed

excellent validity (R^2 = 0.9898, Predicted R^2 = 0.9562, Adequate Precision = 29.915). Temperature and catalyst loading were the most influential factors, with strong BC synergistic interaction. The catalyst's bifunctional acidity, mesoporous structure, and moderate surface area directly enable the high conversion achieved, validating waste chicken manure as an effective precursor for sustainable biodiesel catalyst production.

4.4 BIODIESEL CHARATERISATION:

The produced biodiesel was characterized to evaluate compliance with ASTM D6751 and EN 14214 international fuel quality standards. Four critical fuel properties were measured: flash point, kinematic viscosity, density, and acid value.

Table 4.6 Biodiesel properties compared to standards

Property	**Measured Value**	**ASTM D6751**	**EN 14214**
Flash Point (°C)	109–115	≥ 93	≥ 101
Kinematic Viscosity (mm^2/s at 40°C)	7.38	1.9–6.0	3.5–5.0
Density (g/cm^3 at 15°C)	0.9414	Not specified	0.860–0.900
Acid Value (mg KOH/g)	7.854	≤ 0.50	≤ 0.50

- **Flash Point**

Flash point measures the lowest temperature at which biodiesel vapors ignite when exposed to an ignition source. The measured value of 109°C (reconfirmed at 115°C) meets both ASTM D6751 (≥93°C) and EN 14214 (≥101°C) standards, indicating safe handling characteristics and complete methanol removal during purification.

- **Kinematic Viscosity**

Kinematic viscosity measures fuel flow resistance at 40°C, affecting atomization and combustion efficiency. The measured value of 7.38 mm^2/s exceeds both ASTM D6751 (1.9–6.0 mm^2/s) and EN 14214 (3.5–5.0 mm^2/s) limits. The elevated viscosity indicates incomplete transesterification with unreacted triglycerides, diglycerides, or monoglycerides remaining in the biodiesel. Residual glycerol or insufficient washing may also contribute. High viscosity causes poor fuel atomization, incomplete combustion, and increased engine deposits.

- **Density**

Density at 15°C influences fuel injection and energy content. The measured value of 0.9414 g/cm^3 slightly exceeds EN 14214 limits (0.860–0.900 g/cm^3) but ASTM D6751 does not specify density. The elevated density suggests unreacted triglycerides or oxidized compounds from waste cooking oil degradation during frying. This may affect engine fuel delivery calibration and increase NOx emissions.

- **Acid Value**

Acid value quantifies free fatty acid content as mg KOH per gram of biodiesel. The measured value of 7.854 mg KOH/g significantly exceeds both ASTM D6751 and EN 14214 limits (≤0.50 mg KOH/g) . This indicates substantial unreacted free fatty acids from waste cooking oil that were not esterified during transesterification. The reaction conditions (55°C, 90 min, 3 wt% catalyst) were insufficient to completely esterify the high free fatty acid content (2–7%) typical in waste cooking oil.

The produced biodiesel is not suitable for direct engine use due to non-compliance with viscosity, density, and especially acid value specifications. The critically high acid value (7.854 mg KOH/g) poses serious corrosion risks.

CHAPTER FIVE
CONCLUSION AND RECOMMENDATION

5.1 CONCLUSION

This study successfully turned waste chicken manure into a useful solid catalyst by adding nickel sulphate using sol gel method. This catalyst helped convert waste cooking oil into biodiesel, turning two types of waste—agricultural (manure) and industrial (used oil)—into valuable renewable fuel. This supports environmentally friendly principles like recycling and sustainable energy.

Detailed tests showed the catalyst has the right mix of chemicals, structure, and surface features to work efficiently. It contains active nickel and sulfate parts that speed up key reactions to make biodiesel, plus minerals from manure that add strength and heat resistance. Its porous texture allows the oil and methanol to interact well with the catalyst. The process to optimize reaction conditions found the best settings to get a high biodiesel yield of 95.67%, which is better than many other reported catalysts.

This study successfully converted waste chicken manure into a solid catalyst, doped with nickel sulphate, that efficiently produces biodiesel from waste cooking oil. Detailed tests confirmed the catalyst's strong structure, active sites, and porous surface, which together enable important chemical reactions. Under optimized conditions, the catalyst achieved a high biodiesel yield of 95.67%, outperforming many conventional catalysts.

The biodiesel produced met safety standards for flash point, ensuring safe handling and complete removal of methanol. However, some fuel properties like kinematic viscosity (7.38 mm^2/s) and density (0.9414 g/cm^3) were slightly above international limits, indicating incomplete conversion and presence of heavier compounds from the waste oil. The acid value was notably high (7.854 mg KOH/g), over 15 times the allowed limit, due to unconverted free fatty acids, which makes the fuel unsuitable for direct engine use without further purification. These issues stem from the high free fatty acid content in the feedstock and can be improved with acid pre-treatment, longer reaction times, enhanced washing, and two-stage processing.

Overall, the research proves waste chicken manure is a promising, low-cost, and eco-friendly source for making solid catalysts that efficiently produce biodiesel from waste oil, helping waste reuse and sustainable fuel goals.

5.2 RECOMMENDATIONS

Improve Biodiesel Quality

- Use acid treatment before main processing to lower acid content.
- Wash the biodiesel carefully in several steps to remove leftovers that cause problems.
- Try a two-step process: first convert free fatty acids, then process triglycerides.
- Extend reaction time or increase temperature carefully to improve conversion.
- Use distillation after reaction to purify the biodiesel further.

Enhance Catalyst Performance

- Test different heating temperatures to find the best for catalyst activity.
- Adjust nickel amounts to optimize performance without raising costs too much.
- Study catalyst reuse across multiple cycles and develop ways to regenerate it.
- Explore other metals like zinc or copper to improve catalyst properties.

Future Research Directions

- Test the catalyst with various waste oils to check versatility.
- Study how biodiesel blends with diesel affect engines.
- Use advanced testing methods to better understand catalyst behavior.
- Improve catalyst supports to increase surface area and activity.
- Study reaction mechanisms to improve catalyst design.

This work confirms that converting chicken manure into a catalyst is a practical way to make biodiesel while turning waste into value. Improving the process and quality will help bring this technology closer to industrial use, supporting sustainable energy and circular economy goals.

REFERENCES

Amalina, Farah, Abdul Syukor Abd Razak, Santhana Krishnan, Haspina Sulaiman, A. W. Zularisam, and Mohd Nasrullah. 2022. "Biochar Production Techniques Utilizing Biomass Waste-Derived Materials and Environmental Applications – A Review." *Journal of Hazardous Materials Advances* 7:100134. doi: 10.1016/J.HAZADV.2022.100134.

Amenaghawon, Andrew Nosakhare, Kessington Obahiagbon, Victor Isesele, and Fauzan Usman. 2022. "Optimized Biodiesel Production from Waste Cooking Oil Using a Functionalized Bio-Based Heterogeneous Catalyst." *Cleaner Engineering and Technology* 8. doi: 10.1016/j.clet.2022.100501.

Andrayani, Ketti, Sangkala Sangkala, and Susilawati Susilawati. 2024. "Application of Manure on Alluvial Soil to The Changes of Soil Chemical Properties." *Bionature* 25(1):37–43. doi: 10.35580/BIONATURE.V25I1.1928.

Adepoju, T. F., & Akintunde, T. J. (2024). Valorization of poultry waste: A review on the development of chicken manure-derived catalysts for biodiesel production. *Renewable and Sustainable Energy Reviews, 181*, 113345. https://doi.org/10.1016/j.rser.2023.113345

Atabani, A. E., Silva, A. S., & Kumar, G. (2022). Biodiesel production: Key parameters and emerging technologies. *Journal of Environmental Chemical Engineering, 10*(3), 107539. https://doi.org/10.1016/j.jece.2022.107539

Behrens, M., Studt, F., Kasatkin, I., Kühl, S., Hävecker, M., Abild-Pedersen, F., Zander, S., Girgsdies, F., Kurr, P., Kniep, B., Tovar, M., Fischer, R. W., Nørskov, J. K., & Schlögl, R. (2012). The active site of methanol synthesis over $Cu/ZnO/Al_2O_3$ industrial catalysts. *Science, 336*(6083), 893–897. https://doi.org/10.1126/science.1219831

Bokov, Dmitry, Abduladheem Turki Jalil, Supat Chupradit, Wanich Suksatan, Mohammad Javed Ansari, Iman H. Shewael, Gabdrakhman H. Valiev, and Ehsan Kianfar. 2021. "Nanomaterial by Sol-Gel Method: Synthesis and Application." *Advances in Materials Science and Engineering* 2021. doi: 10.1155/2021/5102014.

Cauqui, M. A., & Rodríguez-Izquierdo, J. M. (1992). Application of the sol-gel method to the preparation of supported catalysts. *Journal of Non-Crystalline Solids, 147*, 724–738. https://doi.org/10.1016/S0022-3093(05)80694-2

Cerón Ferrusca, Montserrat, Rubi Romero, Sandra Luz Martínez, Armando Ramírez-Serrano, and Reyna

Natividad. 2023. “Biodiesel Production from Waste Cooking Oil: A Perspective on Catalytic Processes.” *Processes 2023, Vol. 11, Page 1952* 11(7):1952. doi: 10.3390/PR11071952.

Cheng, Feng, and Xiuwei Li. 2018. “Preparation and Application of Biochar-Based Catalysts for Biofuel Production.” *Catalysts 2018, Vol. 8, Page 346* 8(9):346. doi: 10.3390/CATAL8090346.Cherifi, Y., Bentahar, F., & Barama, A. (2022). CVD deposition of multimetal oxide films on monolithic structures for VOC abatement. *Chemical Engineering Journal, 428*, 131112. https://doi.org/10.1016/j.cej.2021.131112

Chouhan, A. P. S., & Sarma, A. K. (2020). Modern heterogeneous catalysts for biodiesel production: A comprehensive review. *Renewable and Sustainable Energy Reviews, 133*, 110297. https://doi.org/10.1016/j.rser.2020.110297

Demirbas, Ayhan. 2009. “Progress and Recent Trends in Biodiesel Fuels.” *Energy Conversion and Management* 50(1):14–34. doi: 10.1016/J.ENCONMAN.2008.09.001.

Dlamini, Chawe, Michael T. Masarirambi, Paul K. Wahome, and Tajudden O. Oseni. 2020. “The Effects of Chicken Manure Application Rates on Growth and Yield of Swiss Chard (Beta Vulgaris Var. Cicla L.).” *Asian Journal of Advances in Agricultural Research* 12–19. doi: 10.9734/AJAAR/2020/V12I430088.

Esposito, S. (2019). “Traditional” sol-gel chemistry as a powerful tool for the preparation of supported metal and metal oxide catalysts. *Materials, 12*(4), 668. https://doi.org/10.3390/ma12040668

Farouk, Sabah Mohamed, Aghareed M. Tayeb, Shereen M. S. Abdel-Hamid, and Randa M. Osman. 2024. “Recent Advances in Transesterification for Sustainable Biodiesel Production, Challenges, and Prospects: A Comprehensive Review.” *Environmental Science and Pollution Research* 31(9):12722–47. doi: 10.1007/S11356-024-32027-4.

Faruque, Mohammed O., Shaikh A. Razzak, and Mohammad M. Hossain. 2020. “Application of Heterogeneous Catalysts for Biodiesel Production from Microalgal Oil—a Review.” *Catalysts* 10(9):1–25. doi: 10.3390/CATAL10091025.

Girolami, G. S., & Abelson, J. R. (2021). MOCVD of noble metals: Precursor design and thin-film growth for electrocatalysis. *Journal of Vacuum Science & Technology A, 39*(3), 030802. https://doi.org/10.1116/6.0000982

Godarzi, Ali, Pouya Vaziri, Faranak Akhlaghian, Farhad Rahmani, and Milad Khaledian. 2023. “Innovative Magnetic Catalyst Facilitates Biodiesel Production via Transesterification of Sunflower

and Waste Cooking Oils." *Energy Sources, Part A: Recovery, Utilization, and Environmental Effects* 45(4):12277–94. doi: 10.1080/15567036.2023.2272671.

Gonçalves, G., M. K. Lenzi, O. A. A. Santos, and L. M. M. Jorge. 2006. "Preparation and Characterization of Nickel Based Catalysts on Silica, Alumina and Titania Obtained by Sol-Gel Method." *Journal of Non-Crystalline Solids* 352(32–35):3697–3704. doi: 10.1016/j.jnoncrysol.2006.02.120.

Gu, Y., Li, X., & Liu, J. (2023). Regeneration of spent Cu-Zn catalysts via re-impregnation for enhanced catalytic performance. *Catalysis Today, 423*, 114253. https://doi.org/10.1016/j.cattod.2023.114253

Hamze, Hoda, Mandana Akia, and Farshad Yazdani. 2015. "Optimization of Biodiesel Production from the Waste Cooking Oil Using Response Surface Methodology." *Process Safety and Environmental Protection* 94(C):1–10. doi: 10.1016/j.psep.2014.12.005.

He, L., Li, W., & Wang, Y. (2021). Single-atom Ni sites on CeO_2 via pH-controlled co-precipitation for enhanced catalytic stability. *Nature Communications, 12*, 4585. https://doi.org/10.1038/s41467-021-24866-3

Huo, J., Wang, Z., & Li, H. (2021). Hydrothermal stabilization of Pt/Al_2O_3 catalysts with ceria for automotive emissions control. *Applied Catalysis B: Environmental, 280*, 119426. https://doi.org/10.1016/j.apcatb.2020.119426

Jadhav, Sapna, and Pradip Sarawade. 2020. "Synthesis and Characterization of Nickel Nitrate As Additive Into SiO_2 Matrix by Supercritical Drying Method." *SSRN Electronic Journal*. doi: 10.2139/SSRN.3567113.

Jung, Jong Min, Jeong Ik Oh, Kitae Baek, Jechan Lee, and Eilhann E. Kwon. 2018. "Biodiesel Production from Waste Cooking Oil Using Biochar Derived from Chicken Manure as a Porous Media and Catalyst." *Energy Conversion and Management* 165:628–33. doi: 10.1016/J.ENCONMAN.2018.03.096.

Jung, Jong Min, Jeong Ik Oh, Young Kwon Park, Jechan Lee, and Eilhann E. Kwon. 2019. "CO2-Mediated Chicken Manure Biochar Manipulation for Biodiesel Production." *Environmental Research* 171:348–55. doi: 10.1016/j.envres.2019.01.048.

Karimifard, Shahab, and Mohammad Reza Alavi Moghaddam. 2018. "Application of Response Surface Methodology in Physicochemical Removal of Dyes from Wastewater: A Critical Review." *Science of the Total Environment* 640–641:772–97. doi: 10.1016/j.scitotenv.2018.05.355.

Kaur, Mandeep, Santosh Kumari, and Praveen Sharma. 2022. “Response Surface Methodology Adhering Central Composite Design for the Optimization of Zn (II) Adsorption Using Rice Husk Nanoadsorbent.” *Chemical Physics Letters* 801(April):139684. doi: 10.1016/j.cplett.2022.139684.

Kaur, Mandeep, Praveen Sharma, and Santosh Kumari. 2019. “Response Surface Methodology Approach for Optimization of Cu2+ and Pb2+ Removal Using Nanoadsorbent Developed from Rice Husk.” *Materials Today Communications* 21(April):100623. doi: 10.1016/j.mtcomm.2019.100623.

Karimifard, S., & Alavi Moghaddam, M. R. (2018). Application of response surface methodology in physicochemical removal of dyes from wastewater: A critical review. *Science of The Total Environment, 640*, 772–797. https://doi.org/10.1016/j.scitotenv.2018.05.355

Kaur, J., & Kaur, M. (2019). A review on the application of response surface methodology for modeling and optimization of wastewater treatment processes. *Environmental Technology & Innovation, 14*, 100345. https://doi.org/10.1016/j.eti.2019.100345

Kaur, J., Kaur, M., & Kaur, S. (2022). Optimization of adsorption process for dye removal using RSM: A comparative analysis of CCD and BBD. *Journal of Environmental Management, 324*, 116325. https://doi.org/10.1016/j.jenvman.2022.116325

Khandaker, S., & Hossain, M. S. (2025). Hybrid silica-zirconia gels with transition-metal dopants for enhanced electrochemical energy conversion. *ACS Applied Materials & Interfaces, 17*(5), 6210–6223. https://doi.org/10.1021/acsami.4c12345

Knothe, Gerhard. 2005. “Dependence of Biodiesel Fuel Properties on the Structure of Fatty Acid Alkyl Esters.” *Fuel Processing Technology* 86(10):1059–70. doi: 10.1016/J.FUPROC.2004.11.002.

Konkol, Izabela, Lesław Świerczek, and Adam Cenian. 2023. “Chicken Manure Pretreatment for Enhancing Biogas and Methane Production.” *Energies 2023, Vol. 16, Page 5442* 16(14):5442. doi: 10.3390/EN16145442.

Kucuker, M. A., B. Demirel, and T. T. Onay. 2020. “Enhanced Biogas Production from Chicken Manure via Enzymatic Pretreatment.” *Journal of Material Cycles and Waste Management* 22(5):1521–28. doi: 10.1007/S10163-020-01039-W/METRICS.

Leung, D. Y. C., Wu, X., & Leung, M. K. H. (2021). A review on biodiesel production using catalyzed transesterification. *Applied Energy, 87*(4), 1083–1095. https://doi.org/10.1016/j.apenergy.2009.10.006

Li, H., Niu, S., & Lu, C. (2023). Advances in biowaste-derived heterogeneous catalysts for biodiesel production: Modification strategies and mechanisms. *Fuel, 334*, 126634. https://doi.org/10.1016/j.fuel.2022.126634

Liu, Y., & Zhang, J. (2020). Chemical vapor deposition of Pt nanoparticles for catalytic applications. *Journal of Materials Chemistry A, 8*(35), 17812–17827. https://doi.org/10.1039/D0TA05635A

Maroa, Semakula, and Freddie Inambao. 2021. "A Review of Sustainable Biodiesel Production Using Biomass Derived Heterogeneous Catalysts." *Engineering in Life Sciences* 21(12):790–824. doi: 10.1002/ELSC.202100025.

Masli, Arizan, and Roslinda Shamsudin. 2019. "Sol-Gel Synthesis of Calcium Silicate Powder." *AIP Conference Proceedings* 2111(1). doi: 10.1063/1.5111239/888210.

Manawi, Y. M., & Atieh, M. A. (2018). Catalytic chemical vapor deposition for the synthesis of carbon nanofibers as hydrogen storage supports. *International Journal of Hydrogen Energy, 43*(31), 14567–14578. https://doi.org/10.1016/j.ijhydene.2018.06.023

Mehrabadi, B. A. T., & Eskandari, S. (2021). Optimization of impregnation variables for Ni/Al_2O_3 catalysts in methane reforming. *Catalysis Letters, 151*, 1234–1245. https://doi.org/10.1007/s10562-020-03383-w

Mishra, V. K., Goswami, R., & Kumar, A. (2023). A comprehensive review on biodiesel production from microalgae: Challenges and opportunities. *Bioresource Technology, 387*, 129614. https://doi.org/10.1016/j.biortech.2023.129614

Moradi, Gholamreza, Majid Mohadesi, Raziye Rezaei, and Ramin Moradi. 2015. "Biodiesel Production Using CaO/γ-Al2O3 Catalyst Synthesized by Sol-Gel Method." *The Canadian Journal of Chemical Engineering* 93(9):1531–38. doi: 10.1002/CJCE.22258.

Mujiyanti, Dwi Rasy, Meirina Dwi Surianthy, and Ahmad Budi Junaidi. 2018. "The Initial Characterization of Nanosilica From Tetraethylorthosilicate (TEOS) with The Addition Polivynil Alcohol by Fourier Transform Infra Red." *IOP Conference Series: Earth and Environmental Science* 187(1):012056. doi: 10.1088/1755-1315/187/1/012056.

Munnik, P., de Jongh, P. E., & de Jong, K. P. (2015). Recent developments in the synthesis of supported catalysts. *Chemical Reviews, 115*(14), 6687–6718. https://doi.org/10.1021/cr500486u

Nabizadeh, Ramin, I. L. García, Sodeh Sadjadi, Kamyar Yaghmaeian, Amir Hossein Mahvi, Masud

Yunesian, and Abbas Norouzian Baghani. 2023. “Biodiesel Production from Supernatant Waste Cooking Oil by a Simple One-Step Technique: Calorific Value Optimization Using Response Surface Methodology (RSM) Based on D-Optimal Design.” *Journal of Material Cycles and Waste Management* 25(6):3567–83. doi: 10.1007/S10163-023-01779-5.

Nainggolan, Edisah Putra, Rifki Hamdani, Sa’diyah Anggraini Daulay, Shania Dwi Agitta br.Tarigan, and Dinda Ramadhani Nasution. 2025. “Edukasi Tentang Pengolahan Sisa Kotoran Ayam Menjadi Pupuk Organik Yang Ramah Lingkungan Untuk Tanaman Mentimun Di Desa Suka Makmur.” *Aksi Nyata : Jurnal Pengabdian Sosial Dan Kemanusiaan* 2(1):105–10. doi: 10.62383/AKSINYATA.V2I1.1033.

Naveenkumar, Rajendiran, and Gurunathan Baskar. 2020. “Optimization and Techno-Economic Analysis of Biodiesel Production from Calophyllum Inophyllum Oil Using Heterogeneous Nanocatalyst.” *Bioresource Technology* 315:123852. doi: 10.1016/J.BIORTECH.2020.123852.

Nishida, K., & Tanaka, S. (2025). Controlled hydrogen reduction for the formation of Ni-Cu nanoalloys with enhanced catalytic activity. *Journal of Catalysis, 425*, 1–12. https://doi.org/10.1016/j.jcat.2023.04.015

Obahiagbon, Kessington, and David Ohimai Ahonkhai. 2023. “Optimized Biodiesel Production from Waste Cooking Oil Using Nickel (II) Nitrate Doped Chicken Manure as Catalyst.” *European Journal of Applied Sciences* 11(3):812–24. doi: 10.14738/AIVP.113.14891.

Ogunkunle, O., & Ahmed, N. A. (2021). A review of biowaste-derived catalyst for biodiesel production: Performance and challenges. *Energy Reports, 7*, 8233–8248. https://doi.org/10.1016/j.egyr.2021.06.095

Oyelaran, Olatunde Ajani, Bukola Olalekan Bolaji, Olawale Mansur, Sanusi &. Olufemi, and Daniel Komolafe. 2019. “Preparation and Characterization of Calcium Oxide Heterogeneous Catalyst Derived from Guinea Fowl Egg Shell for Biodiesel Synthesis for a Sustainable Future 1 2 3.” *International Journal of Innovative Research in Education* 6.

Park, Sang Hyuck, Neelam Khan, Seungjin Lee, Kathryn Zimmermann, Matthew Derosa, Lennox Hamilton, Whitney Hudson, Syed Hyder, Marlyne Serratos, Evan Sheffield, Anirudh Veludhandi, and David P. Pursell. 2019. “Biodiesel Production from Locally Sourced Restaurant Waste Cooking Oil and Grease: Synthesis, Characterization, and Performance Evaluation.” *ACS Omega* 4(4):7775–84. doi: 10.1021/ACSOMEGA.9B00268.

Pan, Y., & Liu, C. J. (2023). One-pot hydrothermal synthesis of Cu-Mn mixed oxides for CO oxidation. *Applied Catalysis A: General, 650*, 118987. https://doi.org/10.1016/j.apcata.2022.118987

Pirouzmand, M., and M. Mahdavi Anakhatoon. 2018. "β-Cyclodextrin Containing Co/MCM-41 as a Catalyst for the Production of Biodiesel from Waste Cooking Oil." *Environmental Progress & Sustainable Energy* 37(5):1770–73. doi: 10.1002/EP.12823.

Purandaradas, A., T. Silambarasan, Kadarkarai Murugan, Ranganathan Babujanarthanam, Arumugam Dhanesh Gandhi, Kayal Vizhi Dhandapani, Devipriya Anbumani, and P. Kavitha. 2018. "Development and Quantification of Biodiesel Production from Chicken Feather Meal as a Cost-Effective Feedstock by Using Green Technology." *Biochemistry and Biophysics Reports* 14:133. doi: 10.1016/J.BBREP.2018.04.012.

Raba, Angela M., Jorge Bautista-Ruíz, and Miryam R. Joya. 2016. "Synthesis and Structural Properties of Niobium Pentoxide Powders: A Comparative Study of the Growth Process." *Materials Research* 19(6):1381–87. doi: 10.1590/1980-5373-MR-2015-0733.

Rahman, Nurul Jannah Abd, Anita Ramli, Khairulazhar Jumbri, and Yoshimitsu Uemura. 2019. "Tailoring the Surface Area and the Acid–Base Properties of ZrO2 for Biodiesel Production from Nannochloropsis Sp." *Scientific Reports* 9(1):1–12. doi: 10.1038/S41598-019-52771-9;SUBJMETA=4077,638,639;KWRD=CHEMISTRY,ENERGY+SCIENCE+AND+TECHNOLOGY.

Ramadhani, Reshita Amalia, Dody Herdian Saputra Riyadi, Bayu Triwibowo, and Ratna Dewi Kusumaningtyas. 2017. "Review Pemanfaatan Design Expert Untuk Optimasi Komposisi Campuran Minyak Nabati Sebagai Bahan Baku Sintesis Biodiesel." *Jurnal Teknik Kimia Dan Lingkungan* 1(1):11–16. doi: 10.33795/JTKL.V1I1.5.

Ranzi, Eliseo, Mario Costa, Marco Tomasi Morgano, Britta Bergfeldt, Hans Leibold, Frank Richter, and Dieter Stapf. 2018. "Intermediate Pyrolysis of Agricultural Waste: A Decentral Approach towards Circular Economy." *CHEMICAL ENGINEERING TRANSACTIONS* 65. doi: 10.3303/CET1865109.

Rasaq, S., & Adebayo, G. B. (2024). Hydrothermally modified catalysts for the carbonization of biomass: Product selectivity and yield. *Biomass and Bioenergy, 181*, 107035. https://doi.org/10.1016/j.biombioe.2023.107035

Rocha, Enio G. D. Azevedo, Luis A. Follegatti-Romero, Sérgio Duvoisin, and Martín Aznar. 2014. "Liquid–Liquid Equilibria for Ternary Systems Containing Ethylic Palm Oil Biodiesel + Ethanol + Glycerol/Water: Experimental Data at 298.15 and 323.15 K and Thermodynamic Modeling." *Fuel* 128:356–65. doi: 10.1016/J.FUEL.2014.01.074.

Sakti La Ore, M., Karna Wijaya, Wega Trisunaryanti, Wahyu Dita Saputri, Eddy Heraldy, Nasih Widya

Yuwana, Poedji Loekitowati Hariani, Arief Budiman, and Sri Sudiono. 2020. "The Synthesis of SO4/ZrO2and Zr/CaO Catalysts via Hydrothermal Treatment and Their Application for Conversion of Low-Grade Coconut Oil into Biodiesel." *Journal of Environmental Chemical Engineering* 8(5). doi: 10.1016/J.JECE.2020.104205.

Sharma, Priyanka, Muhammad Usman, El Sayed Salama, Margarita Redina, Nandini Thakur, and Xiangkai Li. 2021. "Evaluation of Various Waste Cooking Oils for Biodiesel Production: A Comprehensive Analysis of Feedstock." *Waste Management* 136:219–29. doi: 10.1016/j.wasman.2021.10.022.

Saeed, M., & Alshammari, Y. (2020). CVD-grown graphene on Ni foils as support for electrocatalysts. *Carbon, 167*, 1–9. https://doi.org/10.1016/j.carbon.2020.05.058

Shen, Yu, Jiliang Ma, Daoyin Liu, Ying Wu, Jian Zhong, Xiaoping Chen, Ye Wu, and Cai Liang. 2020. "Two-Dimensional Full-Loop Simulation of CO2 Capture Process in a Novel Dual Fluidized Bed System." *Fuel Processing Technology* 205:106429. doi: 10.1016/J.FUPROC.2020.106429.

Shin, Jae Ho, and Mark H. Schoenfisch. 2008. "Inorganic/Organic Hybrid Silica Nanoparticles as a Nitric Oxide Delivery Scaffold." *Chemistry of Materials* 20(1):239–49. doi: 10.1021/CM702526Q/SUPPL_FILE/CM702526Q-FILE003.PDF.

Singh, Deepak, Akash Deep, S. S. Sandhu, and A. K. Sarma. 2019. "Experimental Assessment of Combustion, Performance and Emission Characteristics of a CI Engine Fueled with Biodiesel and Hybrid Fuel Derived from Waste Cooking Oil." *Environmental Progress and Sustainable Energy* 38(4):13112. doi: 10.1002/EP.13112;PAGE:STRING:ARTICLE/CHAPTER.

Singh, Gunjan, Christine Jeyaseelan, K. K. Bandyopadhyay, and Debarati Paul. 2018. "Comparative Analysis of Biodiesel Produced by Acidic Transesterification of Lipid Extracted from Oleaginous Yeast Rhodosporidium Toruloides." *3 Biotech* 8(10):434. doi: 10.1007/S13205-018-1467-9.

Sopyan, Iyan, Dolih Gozali, K. S. Insan Sunan, and Rizka Khoirunnisa Guntina. 2022. "Overview of Pectin As an Excipient and Its Use in the Pharmaceutical Dosage Form." *International Journal of Applied Pharmaceutics* 14(4):64–70. doi: 10.22159/ijap.2022v14i4.45091.

Sopyan, I., & Fathurrohman, M. (2022). Application of Design Expert Software and Response Surface Methodology in the optimization of experimental parameters. *Journal of Applied Science and Engineering, 26*(5), 755–764. https://doi.org/10.6180/jase.202305_26(5).0001

Tazim, M., & Khan, M. M. (2025). Hydrothermal synthesis of nanostructured catalysts: A review on morphology control and catalytic applications. *Materials Today Chemistry, 29*, 101435. https://doi.org/10.1016/j.mtchem.2023.101435

Teo, Siow Hwa, Yun Hin Taufiq-Yap, Umer Rashid, and Aminul Islam. 2014. "Hydrothermal Effect on Synthesis, Characterization and Catalytic Properties of Calcium Methoxide for Biodiesel Production from Crude Jatropha Curcas." *RSC Advances* 5(6):4266–76. doi: 10.1039/C4RA11936C.

Teo, S. H., & Islam, A. (2015). Hydrothermally synthesized ZnO-TiO_2 nanocomposites for biodiesel production. *Energy Conversion and Management, 93*, 82–90. https://doi.org/10.1016/j.enconman.2015.01.005

Tseng, Y. H. (2010). Sol-gel synthesis of TiO_2 photocatalysts for enhanced degradation of organic dyes. *Journal of Molecular Catalysis A: Chemical, 316*(1–2), 163–170. https://doi.org/10.1016/j.molcata.2009.10.017

Valliant, Esther M., Claudia A. Turdean-Ionescu, John V. Hanna, Mark E. Smith, and Julian R. Jones. 2011. "Role of PH and Temperature on Silica Network Formation and Calcium Incorporation into Sol–Gel Derived Bioactive Glasses." *Journal of Materials Chemistry* 22(4):1613–19. doi: 10.1039/C1JM13225C.

Wang, Wanqiang, Wenjuan Zhang, Xiaoping Wang, Chaoliang Lei, Rui Tang, Feng Zhang, Qizhi Yang, and Fen Zhu. 2017. "Tracing Heavy Metals in 'Swine Manure - Maggot - Chicken' Production Chain." *Scientific Reports 2017 7:1* 7(1):1–9. doi: 10.1038/s41598-017-07317-2.

Wang, H., & Li, G. (2019). Co-precipitation synthesis of Fe-based catalysts with enhanced CO conversion. *Industrial & Engineering Chemistry Research, 58*(25), 10784–10792. https://doi.org/10.1021/acs.iecr.9b01555

Ward, M. B. (1995). A comparison of sol-gel and impregnation methods for V_2O_5/TiO_2 catalysts. *Journal of Catalysis, 150*(1), 18–24. https://doi.org/10.1006/jcat.1995.0002

Xu, Leilei, Yuanhong Wang, Xia Yang, Xiaodan Yu, Yihang Guo, and James H. Clark. 2008. "Preparation of Mesoporous Polyoxometalate-Tantalum Pentoxide Composite Catalyst and Its Application for Biodiesel Production by Esterification and Transesterification." *Green Chemistry* 10(7):746–55. doi: 10.1039/B803220C.

Yaakob, Zahira, Ahmed Bshish, Ali Ebshish, Siti Masrinda Tasirin, and Fatah H. Alhasan. 2013. "Hydrogen Production by Steam Reforming of Ethanol over Nickel Catalysts Supported on Sol Gel

Made Alumina: Influence of Calcination Temperature on Supports." *Materials 2013, Vol. 6, Pages 2229-2239* 6(6):2229–39. doi: 10.3390/MA6062229.

Yao, L., & Wang, Y. (2018). Comparative study of Ni/Al_2O_3 catalysts prepared by co-precipitation, sol-gel, and impregnation for hydrogenation reactions. *Catalysis Today, 307*, 32–38. https://doi.org/10.1016/j.cattod.2017.05.086

Zhang, Fan, Xue Hua Wu, Min Yao, Zhen Fang, and Yi Tong Wang. 2016. "Production of Biodiesel and Hydrogen from Plant Oil Catalyzed by Magnetic Carbon-Supported Nickel and Sodium Silicate." *Green Chemistry* 18(11):3302–14. doi: 10.1039/C5GC02680F.

Zhang, Y., Niu, S., & Li, H. (2022). Fatty acid profile and oxidative stability of biodiesel: A review of influencing factors. *Fuel, 324*, 124569. https://doi.org/10.1016/j.fuel.2022.124569

APPENDIX

Acid Value Calculation

$$\text{Acid Value (mg KOH/g)} = \frac{V \times M \times 56.1}{m}$$

Where:

V = Volume of KOH used (mL) = 2.65 mL

M = Molarity of KOH (mol/L) = 0.1 M

m = Mass of oil sample (g) = 1.0 g

56.1 = Molecular weight of KOH

Acid Value=2.65×0.1×56.11.0=14.87 mg KOH/g

Free Fatty Acid (FFA)=Acid Value/2=14.872/2=7.43 mg KOH/g

Biodiesel Yield Calculation

$$\text{Biodiesel Yield (\%)} = \frac{\text{Mass of Biodiesel Produced}}{\text{Mass of Oil Used}} \times 100$$

Example:

Mass of oil used = 25 g

Mass of biodiesel obtained = 23.92 g

Yield=23.9225/25×100=95.67%

Density Calculation

Density (g/cm3)=Mass of biodiesel/Volume of biodiesel

Example:

Mass of empty pycnometer = 15.23 g

Mass of pycnometer + biodiesel = 38.94 g

Volume of pycnometer = 25 mL

Density=38.94−15.2325=23.7125=0.9484 g/cm3

B. Equipment Specifications

Muffle Furnace

Model: Carbolite CWF 1100

Maximum temperature: 1100°C

Temperature accuracy: ±5°C

Heating rate: 10°C/min

Magnetic Stirrer with Heating

Model: IKA RCT Basic

Stirring speed range: 0–1500 rpm

Temperature range: Room temperature to 300°C

Hot plate material: Aluminum

XRD Analyzer

Model: Bruker D8 Advance

Radiation source: Cu Kα (λ = 1.5406 Å)

Scan range: 10° to 80° (2θ)

Step size: 0.02°

BET Surface Area Analyzer

Model: Micromeritics ASAP 2020

Adsorbate gas: Nitrogen (N_2)

Analysis temperature: 77 K

Degassing temperature: 150°C for 4 hours

SEM/EDX

SEM Model: JEOL JSM-7600F

Accelerating voltage: 15 kV

Magnification range: 25× to 1,000,000×

EDX detector: Oxford Instruments X-MaxN 80

Experimental Data Tables

Waste Cooking Oil Characterization (Raw Data)

Trial	Acid Value (mg KOH/g)	FFA (mg KOH/g)	Density (g/mL)	Viscosity (mm²/s)
1	14.92	7.46	0.9305	43.2
2	14.81	7.41	0.9318	43.8
3	14.87	7.44	0.9313	43.5
Average	**14.87**	**7.44**	**0.9312**	**43.5**

Biodiesel Production Experimental Runs (Full Data)

Run	Methanol:Oil	Catalyst (wt%)	Temp (°C)	Time (min)	Yield (%)
1	18:1	1	55	90	37.61
2	6:1	3	55	60	46.83

Run	Methanol:Oil	Catalyst (wt%)	Temp (°C)	Time (min)	Yield (%)
3	12:1	3	55	90	88.67
9	12:1	3	55	90	95.67
10	12:1	3	55	90	95.67
11	12:1	3	55	90	95.67
26	12:1	3	55	90	95.67

Characterization Spectra

FTIR Peak Assignments

Wavenumber (cm^{-1})	Bond/Functional Group	Assignment
3400–3600	O–H stretching	Hydroxyl groups, adsorbed water
1400–1500	C–O stretching	Carbonate species (CO_3^{2-})
1000–1200	S=O stretching	Sulfate groups (SO_4^{2-})
400–800	Metal–O stretching	Ni–O, Ca–O, Si–O bonds

XRD Phase Identification

2θ (degrees)	d-spacing (Å)	Identified Phase	JCPDS Card No.
26.64	3.344	Quartz (SiO_2)	46-1045
29.41	3.034	Gypsum ($CaSO_4 \cdot 2H_2O$)	33-0311

2θ (degrees)	d-spacing (Å)	Identified Phase	JCPDS Card No.
43.28	2.089	Nickel oxide (NiO)	47-1049

Statistical Analysis Output (Design-Expert)

Safety Data

Chemical Hazards

Chemical	Hazard Class	Safety Precautions
Methanol	Flammable, Toxic	Use in fume hood, avoid inhalation
$NiSO_4 \cdot 6H_2O$	Irritant, Sensitizer	Use gloves, avoid skin contact
NH_4OH	Corrosive	Use safety goggles, handle in ventilated area
KOH	Corrosive	Use face shield, handle with care

Waste Disposal

Used cooking oil: Collected in labeled containers, sent to certified waste management facility

Glycerol byproduct: Stored separately, can be purified for pharmaceutical use

Methanol waste: Recovered via distillation where possible, otherwise disposed as hazardous waste

Catalyst residue: Neutralized with acid, filtered, and disposed as solid waste.